

TIT/HEP-445

hep-th/0004188

April, 2000

Nonnormalizable Zero Modes on BPS Junctions

KENJI ITO,^{*} MASASHI NAGANUMA,[†] HODAKA ODA,[‡] and NORISUKE SAKAI[§]*Department of Physics, Tokyo Institute of Technology**Oh-okayama, Meguro, Tokyo 152-8551, Japan*

Abstract

Using an exact solution as a concrete example, Nambu-Goldstone modes on the BPS domain wall junction are worked out for $\mathcal{N} = 1$ supersymmetric theories in four dimensions. Their wave functions extend along the wall to infinity (not localized) and are not normalizable. It is argued that this feature is a generic phenomenon of Nambu-Goldstone modes on domain wall junctions in the bulk flat space in any dimensions. We formulate mode equations and show that fermion and boson with the same mass come in pairs except massless modes which can appear singly, in accordance with unitary representations of $(1, 0)$ supersymmetry.

PACS number(s): 11.27.+d, 11.30.P, 11.15.Kc, 11.10.-z

^{*} e-mail: kito@th.phys.titech.ac.jp

[†] e-mail: naganuma@th.phys.titech.ac.jp

[‡] e-mail: hoda@th.phys.titech.ac.jp

[§] e-mail: nsakai@th.phys.titech.ac.jp

1 Introduction

In recent years an interesting idea has been advocated to regard our world as a domain wall embedded in higher dimensional spacetime [1]. Most of the particles in the standard model should be realized as modes localized on the wall. Phenomenological implications of the idea have been extensively studied from many aspects. Another fascinating possibility has also been proposed to consider walls in the bulk spacetime which has negative cosmological constant [2]. The model can give large mass hierarchy or can give massless graviton localized on the wall. Subsequently a great deal of research activity has been performed to study and extend the proposal [4].

Since walls typically have co-dimension one, it is desirable to consider intersections and/or junctions of walls in order to obtain our four dimensional world from a spacetime with much higher dimensions. The model with the bulk cosmological constant has been extended to produce an intersection of walls [3].

Supersymmetry has been useful to achieve stability of solitonic solutions such as domain walls. Domain walls in supersymmetric theories can saturate the Bogomol'nyi bound [5]. Such a domain wall preserves half of the original supersymmetry and is called a 1/2 BPS state [6]. It has also been noted that these BPS states possess a topological charge which becomes a central charge Z of the supersymmetry algebra [7] [8]. Thanks to the topological charge, these BPS states are guaranteed to be stable under arbitrary local fluctuations. Various properties of domain walls in $\mathcal{N} = 1$ supersymmetric field theories in four dimensions have been extensively studied [9], [10]. In particular the modes on the domain wall background have been worked out and are found to contain fermions and/or bosons localized on the wall in many cases [11], [12].

Recently domain wall junctions have attracted much attention as another interesting possibility for BPS states [13]–[15]. Domain walls occur in interpolating two discrete degenerate vacua in separate region of space. If three or more different discrete vacua occur in separate region of space, segments of domain walls separate each pair of the neighboring vacua. If the two spatial dimensions of all of these domain walls have one dimension in common, these domain walls meet at a one-dimensional junction. The solitonic configuration for the junction can preserve a quarter of supersymmetry and is called a 1/4 BPS state. There has been progress to study general properties of such domain wall junctions. For instance a new topological charge Y is found to appear for such a 1/4 BPS state [13]–[15]. If we start from $\mathcal{N} = 1$ four dimensional supersymmetric field theories, the domain wall junction preserves only one supercharge. Consequently the resulting theory was expected to be a $(1, 0)$ supersymmetric theory in $1 + 1$ dimensions [13] which offers an intriguing possibility of chiral fermions. Moreover, there have been a number of numerical simulations which indicate the existence of the domain wall junction solutions [16]. In spite of all these efforts, it has been difficult to obtain an explicit solution and to prove the existence of a BPS domain wall junction.

Recently we have succeeded to work out an exact solution for the BPS domain wall junction for the first time [17]. The exact solution allows a thorough study of the properties of the BPS domain wall junction. Consequently several misconceptions can be pointed out and rectified. One such point is the sign and meaning of the new central charge Y which arises when walls

form a junction. Our exact solution showed that the central charge Y contributes negatively to the mass of the domain wall junction configuration. Therefore we should not consider the central charge Y alone as the mass of the junction. Various other aspects of the domain wall junctions are also studied recently [21] – [23].

The purpose of the present paper is to give a more detailed study of the properties of the BPS domain wall junction in $\mathcal{N} = 1$ supersymmetric field theories. We study the modes on the background of the domain wall junction, especially the Nambu-Goldstone modes. We will use our exact solution as a concrete example and will extract the generic properties of the BPS domain wall junctions. We define mode equations and demonstrate explicitly that fermion and boson with the same mass have to come in pairs except massless modes. Massless modes can appear singly without accompanying fields with opposite statistics. We also show that unitary representations of the surviving $(1,0)$ supersymmetry are classified into doublets for massive modes and singlets for massless modes. We work out explicitly massless Nambu-Goldstone modes associated with the broken supersymmetry and translational invariance. We find that the Nambu-Goldstone fermions exhibit an interesting chiral structure in accordance with the surviving $(1,0)$ supersymmetry algebra. However, we also find that any linear combinations of the Nambu-Goldstone modes associated with the junctions become a linear combination of zero modes on at least one of the domain walls asymptotically along these walls. Since their wave functions are extended along these walls without damping, they are not localized states on the junction. Therefore they are not normalizable, contrary to a previous expectation [13]. This indicates that the resulting theory cannot be regarded as a genuine $1 + 1$ dimensional field theory with discrete particle spectrum even at zero energy. Although the remaining supersymmetry is just $(1,0)$ which is characteristic to $1 + 1$ dimensions, we have to keep in mind that the domain wall junction configuration is actually living in one more dimensions similarly to the domain wall itself. Zero modes on the junction turn out to have properties quite similar to those on the domain wall. The non-normalizability of Nambu-Goldstone modes on the junction configuration is not an accident in this particular model. We observe that the origin of this property can be traced back to the fact that the supersymmetry is broken by the coexistence of nonparallel walls. Therefore the fact that the Nambu-Goldstone modes on the BPS domain wall junction are not normalizable is a generic feature of supersymmetric field theories in the bulk flat space.

One should note that our conclusion need not apply to the case with negative cosmological constant in the bulk. In the presence of a bulk negative cosmological constant in six dimensions, five dimensional walls can intersect in Anti de Sitter space. If one demands a flat space at the four dimensional intersection, one has an Anti de Sitter space not only in the bulk but also even on the walls [3]. Since Anti de Sitter space does not have translational invariance, the wave function of the zero mode does not become constant along the wall asymptotically, contrary to our situation. If one approaches the intersection along the wall, one meets precisely the same situation as the wall in the five dimensional Anti de Sitter space. For instance graviton zero mode is exponentially suppressed away from the intersection along the wall direction to produce a normalizable wave function. Therefore the Anti de Sitter geometry along the wall plays an essential role to achieve the localization of the wave function on the intersection in models with cosmological constant.

In sect. 2, we introduce BPS equations and the exact solution for the domain wall junction and

discuss representations of the surviving $(1, 0)$ supersymmetry algebra. In sect. 3, we present mode equations which define the fluctuations on the background of domain wall junction. We work out the Nambu-Goldstone mode explicitly and show that they are not normalizable. Physical origin of the nonnormalizability is clarified and the general validity of this phenomenon is argued. In sect. 4, the relation between the choice of BPS equations and the boundary condition is discussed for a general Wess-Zumino model. In sect. 5, the central charge density and the energy density are examined and an interesting behavior is observed. The fermionic contributions to the central charges and mode equations in a convenient gamma matrix representation are given in appendices.

2 BPS equations and the $(1, 0)$ supersymmetry algebra

2.1 Two $1/4$ BPS states and two BPS equations

It is known that if the translational invariance is broken as is the case for domain walls and/or junctions, the $\mathcal{N} = 1$ superalgebra in general receives contributions from central charges [18], [8]–[17], [19]. The anti-commutator between two left-handed supercharges has central charges Z_k , $k = 1, 2, 3$

$$\{Q_\alpha, Q_\beta\} = 2i(\sigma^k \bar{\sigma}^0)_\alpha{}^\gamma \epsilon_{\gamma\beta} Z_k. \quad (2.1)$$

Here and the following we use two-component spinors following the convention of ref.[20] except that the four dimensional indices are denoted by Greek letters $\mu, \nu = 0, 1, 2, 3$ instead of roman letters m, n . The anti-commutator between left- and right-handed supercharges receives a contribution from central charges Y_k , $k = 1, 2, 3$ besides the energy-momentum four-vector P^μ , $\mu = 0, \dots, 3$ of the system

$$\{Q_\alpha, \bar{Q}_{\dot{\alpha}}\} = 2(\sigma_{\alpha\dot{\alpha}}^\mu P_\mu + \sigma_{\alpha\dot{\alpha}}^k Y_k). \quad (2.2)$$

One may call Z_k and Y_k as $(1, 0)$ and $(1/2, 1/2)$ central charges in accordance with the transformation properties under the Lorentz group. Central charges, Z_k and Y_k , come from the total divergence, and they are non-vanishing when there are nontrivial differences in asymptotic behavior of fields in different region of spatial infinity as is the case of domain walls and junctions [14]. Therefore these charges are topological in the sense that they are determined completely by the boundary conditions at infinity. For instance, we can take a general Wess-Zumino model with an arbitrary number of chiral superfields Φ^i , an arbitrary superpotential \mathcal{W} and an arbitrary Kähler potential $K(\Phi^i, \Phi^{*j})$

$$\mathcal{L} = \int d^2\theta d^2\bar{\theta} K(\Phi^i, \Phi^{*j}) + \left[\int d^2\theta \mathcal{W}(\Phi^i) + \text{h.c.} \right], \quad (2.3)$$

and compute the anticommutators (2.1), (2.2) to find the central charges. The contributions to these central charges from bosonic components of chiral superfields are given * by [14]

$$Z_k = 2 \int d^3x \partial_k \mathcal{W}^*(A^*), \quad (2.4)$$

$$Y_k = i\epsilon^{knm} \int d^3x K_{ij^*} \partial_n (A^{*j} \partial_m A^i), \quad \epsilon^{123} = 1, \quad (2.5)$$

where A^i is the scalar component of the i -th chiral superfield Φ^i and $K_{ij^*} = \partial^2 K(A^*, A) / \partial A^i \partial A^{*j}$ is the Kähler metric.

BPS domain wall is a 1/2 BPS state [8] and BPS domain wall junction is a 1/4 BPS state [13][14]. To find the BPS equations satisfied by these BPS states, we consider a hermitian linear combination of operators Q and \bar{Q} with an arbitrary complex two-vector β^α and its complex conjugate $\bar{\beta}^{\dot{\alpha}} = (\beta^\alpha)^*$ as coefficients

$$K = \beta^\alpha Q_\alpha + \bar{\beta}^{\dot{\alpha}} \bar{Q}_{\dot{\alpha}}. \quad (2.6)$$

We treat β^α as c-numbers rather than the Grassmann numbers. Since K is hermitian, the expectation value of the square of K over any state is non-negative definite, $\langle S | K^2 | S \rangle \geq 0$. The field configuration of static junction must be at least two-dimensional. If we assume, for simplicity, that it depends on x^1, x^2 then we obtain $\langle Z_3 \rangle = \langle Y_1 \rangle = \langle Y_2 \rangle = 0$ from Eqs.(2.4) and (2.5), and the inequality implies in this case

$$\begin{aligned} \langle H \rangle \geq \frac{-1}{|\beta^1|^2 + |\beta^2|^2} & \left\{ (|\beta^1|^2 - |\beta^2|^2) \langle Y_3 \rangle + \text{Re} [(\beta^1)^2 \langle -Z_2 - iZ_1 \rangle] \right. \\ & \left. + \text{Re} [(\beta^2)^2 \langle -Z_2 + iZ_1 \rangle] \right\}, \end{aligned} \quad (2.7)$$

for any β^α and for any state. The equality holds if and only if the linear combination of supercharges, K , is preserved by the state $|S\rangle$

$$K |S\rangle = 0. \quad (2.8)$$

In this case, the state $|S\rangle$ saturates the energy bound and is called a BPS state. We find that there are two candidates for the saturation of the energy bound [17];

$$H = H_I \equiv |\langle -iZ_1 - Z_2 \rangle| - \langle Y_3 \rangle, \quad \text{when } \bar{\beta}^{\dot{1}} = \beta^1 \frac{\langle iZ_1 + Z_2 \rangle}{|\langle iZ_1 + Z_2 \rangle|}, \quad \beta^2 = \bar{\beta}^{\dot{2}} = 0, \quad (2.9)$$

$$H = H_{II} \equiv |\langle iZ_1 - Z_2 \rangle| + \langle Y_3 \rangle, \quad \text{when } \beta^1 = \bar{\beta}^{\dot{1}} = 0, \quad \bar{\beta}^{\dot{2}} = \beta^2 \frac{\langle -iZ_1 + Z_2 \rangle}{|\langle -iZ_1 + Z_2 \rangle|}. \quad (2.10)$$

In the case of $H_I \neq H_{II}$, the BPS bound becomes $\langle H \rangle \geq \max\{H_I, H_{II}\}$. If $H_I > H_{II}$, then supersymmetry can only be preserved at $\langle H \rangle = H_I$ and the only one combination of supercharges is conserved

$$\left(Q_1 + \frac{\langle iZ_1 + Z_2 \rangle}{|\langle iZ_1 + Z_2 \rangle|} \bar{Q}_{\dot{1}} \right) |\langle H \rangle = H_I\rangle = 0. \quad (2.11)$$

*The central charge Y_k also receives contributions from fermionic components of chiral superfields which is given in appendix A.

If $H_{\text{II}} > H_{\text{I}}$, then supersymmetry can only be preserved at $\langle H \rangle = H_{\text{II}}$ and the only one combination of supercharges is conserved

$$\left(Q_2 + \frac{\langle -iZ_1 + Z_2 \rangle}{|\langle -iZ_1 + Z_2 \rangle|} \bar{Q}_2 \right) |\langle H \rangle = H_{\text{II}} \rangle = 0. \quad (2.12)$$

In the case of $H_{\text{I}} = H_{\text{II}}$, two candidates of BPS bounds coincide and BPS state conserves both of two supercharges, (2.11) and (2.12); this is a 1/2 BPS state.

For the general Wess-Zumino model in Eq.(2.3), the condition of supercharge conservation (2.11) for $H = H_{\text{I}}$ applied to chiral superfield $\Phi^i = (A^i, \psi^i, F^i)$ gives after eliminating the auxiliary field F^i

$$2 \frac{\partial A^i}{\partial \bar{z}} = -\Omega_+ F^i = \Omega_+ K^{-1ij*} \frac{\partial \mathcal{W}^*}{\partial A^{*j}}, \quad \Omega_+ \equiv i \frac{\langle -iZ_1^* + Z_2^* \rangle}{|\langle -iZ_1^* + Z_2^* \rangle|}, \quad (2.13)$$

where complex coordinates $z = x^1 + ix^2$, $\bar{z} = x^1 - ix^2$, and the inverse of the Kähler metric K^{-1ij*} are introduced. We can also consider gauge interactions. For simplicity we take only the $U(1)$ gauge interaction. Then the derivative $\partial A^i / \partial \bar{z}$ in the above Eq.(2.13) should be replaced by the gauge covariant derivative $\mathcal{D}_{\bar{z}} A^i$

$$2 \mathcal{D}_{\bar{z}} A^i = \Omega_+ K^{-1ij*} \frac{\partial \mathcal{W}^*}{\partial A^{*j}}, \quad \mathcal{D}_{\bar{z}} = \frac{1}{2} (\mathcal{D}_1 + i\mathcal{D}_2), \quad \mathcal{D}_\mu A^i = \left(\frac{\partial}{\partial x^\mu} + i \frac{e_i}{2} v_\mu \right) A^i. \quad (2.14)$$

Moreover the same BPS condition (2.11) applied to vector superfield in the Wess-Zumino gauge $V = (v_\mu, \lambda, D)$ gives after eliminating the auxiliary field D

$$v_{12} = -D = \frac{1}{2} \sum_j A^{*j} e_j A^j, \quad v_{03} = 0, \quad v_{01} = v_{31}, \quad v_{23} = -v_{02}, \quad (2.15)$$

where $v_{\mu\nu} \equiv \partial_\mu v_\nu - \partial_\nu v_\mu$ and e_j is the charge of the field A^j . Here we assume for simplicity the minimal kinetic term both for the chiral superfield $K_{ij*} = \delta_{ij*}$ and for the vector superfield.

Similarly the condition of supercharge conservation (2.12) for $H = H_{\text{II}}$ applied to chiral superfield in the Wess-Zumino model gives after eliminating the auxiliary field

$$2 \frac{\partial A^i}{\partial z} = -\Omega_- F^i = \Omega_- K^{-1ij*} \frac{\partial \mathcal{W}^*}{\partial A^{*j}}, \quad \Omega_- \equiv i \frac{\langle -iZ_1^* - Z_2^* \rangle}{|\langle -iZ_1^* - Z_2^* \rangle|}. \quad (2.16)$$

If $U(1)$ gauge interaction is present, the derivative $\partial A^i / \partial z$ should be replaced by the covariant derivative $\mathcal{D}_z A^i = \frac{1}{2} (\mathcal{D}_1 - i\mathcal{D}_2) A^i$. In this case the BPS condition applied to $U(1)$ vector superfield in the Wess-Zumino gauge becomes in the case of minimal kinetic terms

$$v_{12} = D = -\frac{1}{2} \sum_j A^{*j} e_j A^j, \quad v_{03} = 0, \quad v_{01} = -v_{31}, \quad v_{23} = v_{02}. \quad (2.17)$$

In sect.4, we shall present a simple way to find the correspondence between the choice of boundary conditions and the choice of BPS equations (2.13) and (2.15) or (2.16) and (2.17).

2.2 The exact solution of BPS domain wall junction

In a previous article [17], we have found an exact solution of BPS domain wall junction in a model motivated by the $\mathcal{N} = 2$ supersymmetric $SU(2)$ gauge theory with one flavor broken to $\mathcal{N} = 1$ by the mass of the adjoint chiral superfield. This model has the following chiral superfields with the charge assignment for the $U(1) \times U(1)'$ gauge group

$$\begin{array}{cccccccc} & \mathcal{M} & \tilde{\mathcal{M}} & \mathcal{D} & \tilde{\mathcal{D}} & \mathcal{Q} & \tilde{\mathcal{Q}} & T \\ U(1) & 0 & 0 & 1 & -1 & 1 & -1 & 0 \\ U(1)' & 1 & -1 & 1 & -1 & 0 & 0 & 0, \end{array} \quad (2.18)$$

interacting with a superpotential

$$\mathcal{W} = (T - \Lambda)\mathcal{M}\tilde{\mathcal{M}} + (T + \Lambda)\mathcal{D}\tilde{\mathcal{D}} + (T - m)\mathcal{Q}\tilde{\mathcal{Q}} - h^2T, \quad (2.19)$$

where parameters Λ and h can be made real positive and a parameter m is complex [17]. In this model there are three discrete vacua,

$$\begin{aligned} \text{Vac.1} : T &= \Lambda, & \mathcal{M} &= \tilde{\mathcal{M}} = h, & \mathcal{Q} &= \tilde{\mathcal{Q}} = \mathcal{D} = \tilde{\mathcal{D}} = 0, & \mathcal{W}_1 &= -h^2\Lambda, \\ \text{Vac.2} : T &= m, & \mathcal{Q} &= \tilde{\mathcal{Q}} = h, & \mathcal{M} &= \tilde{\mathcal{M}} = \mathcal{D} = \tilde{\mathcal{D}} = 0, & \mathcal{W}_2 &= -h^2m, \\ \text{Vac.3} : T &= -\Lambda, & \mathcal{D} &= \tilde{\mathcal{D}} = h, & \mathcal{Q} &= \tilde{\mathcal{Q}} = \mathcal{M} = \tilde{\mathcal{M}} = 0, & \mathcal{W}_3 &= h^2\Lambda, \end{aligned} \quad (2.20)$$

and when $m = i\sqrt{3}\Lambda$, this model becomes Z_3 symmetric. Thus three half walls are expected to connect at the junction with relative angles of $2\pi/3$. For definiteness, we specify the boundary condition where the wall 1 extends along the negative x^2 axis separating the vacuum 1 ($x^1 > 0$) and 3 ($x^1 < 0$) as shown in Fig. 1. If we have only the wall 1, we obtain the central charge Z_k

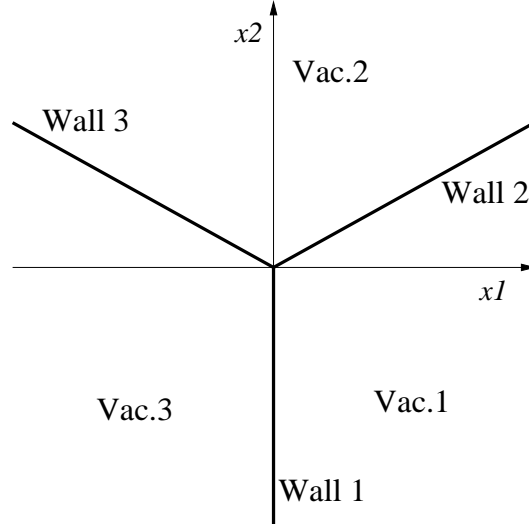


Figure 1: Boundary condition of the model in [17]

(vanishing Y_k) and find the two conserved supercharges from Eqs.(2.11) and (2.12) as

$$Q^{(1)} = \frac{1}{\sqrt{2}}(e^{-i\frac{\pi}{4}}Q_2 + e^{i\frac{\pi}{4}}\overline{Q}_2), \quad Q^{(2)} = \frac{1}{\sqrt{2}}(e^{i\frac{\pi}{4}}Q_1 + e^{-i\frac{\pi}{4}}\overline{Q}_1). \quad (2.21)$$

The other two walls have also two conserved supercharges

$$\begin{aligned} \text{at wall 2} \quad Q^{(3)} &= \frac{1}{\sqrt{2}}(e^{-i\frac{\pi}{12}}Q_1 + e^{i\frac{\pi}{12}}\overline{Q}_1), \text{ besides } Q^{(1)} = \frac{1}{\sqrt{2}}(e^{-i\frac{\pi}{4}}Q_2 + e^{i\frac{\pi}{4}}\overline{Q}_2), \\ \text{at wall 3} \quad Q^{(4)} &= \frac{1}{\sqrt{2}}(e^{-i\frac{5\pi}{12}}Q_1 + e^{i\frac{5\pi}{12}}\overline{Q}_1), \text{ besides } Q^{(1)} = \frac{1}{\sqrt{2}}(e^{-i\frac{\pi}{4}}Q_2 + e^{i\frac{\pi}{4}}\overline{Q}_2). \end{aligned} \quad (2.22)$$

When these three half walls coexist, we can have only one common conserved supercharge $Q^{(1)} = (e^{-i\frac{\pi}{4}}Q_2 + e^{i\frac{\pi}{4}}\overline{Q}_2)/\sqrt{2}$. In fact we find that the domain wall junction configuration conserves precisely this single combination of supercharges, even though it has also another central charge Y_k contributing. Correspondingly we obtain the BPS equations (2.16) and (2.17) for $H = H_{\text{II}}$ with $\Omega_- = -1$. The BPS equations (2.17) for the vector superfield can be trivially satisfied by $v_\mu = 0$ and $D = 0$. The BPS equations (2.16) for chiral superfields become in this case

$$2\frac{\partial A^i}{\partial z} = -\frac{\partial \mathcal{W}^*}{\partial A^{*i}}, \quad (2.23)$$

assuming the minimal kinetic term. The solution for these BPS equations is given by [17],

$$\begin{aligned} \mathcal{M}(z, \bar{z}) &= \tilde{\mathcal{M}}(z, \bar{z}) = \frac{\sqrt{2}\Lambda s}{s+t+u}, \\ \mathcal{D}(z, \bar{z}) &= \tilde{\mathcal{D}}(z, \bar{z}) = \frac{\sqrt{2}\Lambda t}{s+t+u}, \\ \mathcal{Q}(z, \bar{z}) &= \tilde{\mathcal{Q}}(z, \bar{z}) = \frac{\sqrt{2}\Lambda u}{s+t+u}, \\ T(z, \bar{z}) &= \frac{2\Lambda}{\sqrt{3}} \frac{e^{-i\frac{1}{6}\pi}s + e^{-i\frac{5}{6}\pi}t + e^{i\frac{1}{2}\pi}u}{s+t+u} + \frac{i}{\sqrt{3}}\Lambda, \end{aligned} \quad (2.24)$$

$$s = \exp\left(\frac{2\Lambda}{\sqrt{3}}\text{Re}\left(e^{i\frac{1}{6}\pi}z\right)\right), \quad t = \exp\left(\frac{2\Lambda}{\sqrt{3}}\text{Re}\left(e^{i\frac{5}{6}\pi}z\right)\right), \quad u = \exp\left(\frac{2\Lambda}{\sqrt{3}}\text{Re}\left(e^{-i\frac{1}{2}\pi}z\right)\right). \quad (2.25)$$

This model is motivated by the softly broken $\mathcal{N} = 2$ $SU(2)$ gauge theory with one flavor. However, we can simplify the model without spoiling the solvability to obtain a Wess-Zumino model consisting of purely chiral superfields by the following procedure. The vector superfields actually serve to constrain chiral superfields to have the identical magnitude pairwise through $D = 0$ to satisfy the BPS equation (2.17) for vector superfields: $|\tilde{\mathcal{M}}| = |\mathcal{M}|, |\tilde{\mathcal{D}}| = |\mathcal{D}|, |\tilde{\mathcal{Q}}| = |\mathcal{Q}|$. Therefore we can eliminate the vector superfields and reduce the number of chiral superfields by identifying pairwise $\tilde{\mathcal{M}} = \mathcal{M}, \tilde{\mathcal{D}} = \mathcal{D}, \tilde{\mathcal{Q}} = \mathcal{Q}$. Correspondingly we should take the superpotential as

$$\mathcal{W} = \frac{1}{2}(T - \Lambda)\mathcal{M}^2 + \frac{1}{2}(T + \Lambda)\mathcal{D}^2 + \frac{1}{2}(T - i\sqrt{3}\Lambda)\mathcal{Q}^2 - \frac{h^2}{2}T. \quad (2.26)$$

This Wess-Zumino model has the same solution as ours by changing $h^2 \rightarrow h^2/2, \Lambda \rightarrow \sqrt{3}\Lambda/2$. A similar observation has also been made in ref.[22].

2.3 Unitary representations of $(1, 0)$ supersymmetry algebra

Let us examine states on the background of a domain wall junction from the point of view of surviving symmetry. In the case of the BPS states satisfying the BPS equation (2.16) corresponding to $H = H_{\text{II}}$, we have only one surviving supersymmetry charge $Q^{(1)}$, two translation generators H, P^3 , and one Lorentz generator J^{03} , out of the $\mathcal{N} = 1$ four dimensional super Poincaré generators. Since we are interested in excitation modes on the background of the domain wall junction, we define the hamiltonian $H' = H - \langle H \rangle$ measured from the energy $\langle H \rangle$ of the background configuration. By projecting from the supersymmetry algebra (2.1), (2.2) with central charges in four dimensions, we immediately find

$$(Q^{(1)})^2 = H' - P^3. \quad (2.27)$$

We also obtain the Poincaré algebra in $1 + 1$ dimensions

$$[J^{03}, Q^{(1)}] = \frac{i}{2}Q^{(1)}, \quad [J^{03}, H' - P^3] = i(H' - P^3), \quad [J^{03}, H' + P^3] = -i(H' + P^3). \quad (2.28)$$

Other commutation relations are trivial

$$[H' - P^3, H' + P^3] = [H' - P^3, Q^{(1)}] = [H' + P^3, Q^{(1)}] = 0. \quad (2.29)$$

This is precisely the $(1, 0)$ supersymmetry algebra on the domain wall junction as anticipated [13].

To obtain unitary representations, we can diagonalize H' and P^3

$$H'|E, p^3\rangle = E|E, p^3\rangle, \quad P^3|E, p^3\rangle = p^3|E, p^3\rangle, \quad E \geq |p^3|, \quad (2.30)$$

and combine them by means of $Q^{(1)}$. If $E - p^3 > 0$, we can construct bosonic state from fermionic state and vice versa by operating $Q^{(1)}$ on the state.

$$|B\rangle = \frac{1}{\sqrt{E - p^3}}Q^{(1)}|F\rangle, \quad |F\rangle = \frac{1}{\sqrt{E - p^3}}Q^{(1)}|B\rangle. \quad (2.31)$$

Therefore we obtain a doublet representation $(|B\rangle, |F\rangle)$. If $E - p^3 = 0$, operating by $Q^{(1)}$ on the state gives an unphysical zero norm state

$$|Q^{(1)}|E, p^3\rangle|^2 = \langle E, p^3| (Q^{(1)})^2 |E, p^3\rangle = \langle E, p^3| H' - P^3 |E, p^3\rangle = E - p^3 = 0. \quad (2.32)$$

Then the massless right-moving state $|E, p^3 = E\rangle$ is a singlet representation. This singlet state can either be boson or fermion. Thus we find that there are only two types of representations of the $(1, 0)$ supersymmetry algebra, doublet and singlet. We also find that massive modes should appear in pairs of boson and fermion, whereas the massless right-moving mode can appear singly without accompanying a state with opposite statistics. This provides an interesting possibility of a chiral structure for fermions.

If another BPS equation (2.13) corresponding to $H = H_{\text{I}}$ is satisfied instead of Eq. (2.16), we have $(0, 1)$ supersymmetry and the left-moving massless states can appear as singlets.

3 Nambu-Goldstone and other modes on the junction

3.1 Mode equation on the junction

Since the vector superfields have no nontrivial field configurations, Nambu-Goldstone modes have no component of vector superfield. Moreover we can replace our model, if we wish, by another model with purely chiral superfields without spoiling the essential features including the solvability. Consequently we shall neglect vector superfields and consider the general Wess-Zumino model in Eq.(2.3) in the following. For simplicity we assume the minimal kinetic term here $K_{ij^*} = \delta_{ij^*}$.

Let us consider quantum fluctuations A^i, ψ^i around a classical solution A_{cl}^i which satisfies the BPS equations (2.13) and (2.15) for $H = H_I$ or (2.16) and (2.17) for $H = H_{II}$.

$$A^i = A_{\text{cl}}^i + A'^i. \quad (3.33)$$

We retain the part of the Lagrangian quadratic in fluctuations and eliminate the auxiliary fields F^i to obtain the linearized equation for the scalar fluctuations

$$-\partial_\mu \partial^\mu A'^{*i} + \frac{\partial^2 \mathcal{W}}{\partial A_{\text{cl}}^i \partial A_{\text{cl}}^k} \frac{\partial^2 \mathcal{W}^*}{\partial A_{\text{cl}}^{*k} \partial A_{\text{cl}}^{*j}} A'^{*j} + \frac{\partial^3 \mathcal{W}}{\partial A_{\text{cl}}^i \partial A_{\text{cl}}^k \partial A_{\text{cl}}^j} \frac{\partial \mathcal{W}^*}{\partial A_{\text{cl}}^{*k}} A'^j = 0. \quad (3.34)$$

In order to separate variables in x^0, x^3 and x^1, x^2 we have to define mode equations on the background which has a nontrivial dependence in two dimensions, x^1, x^2 . The bosonic modes $A_n^i(x^1, x^2)$ can easily be defined in terms of a differential operator \mathcal{O}_B in x^1, x^2 space

$$\mathcal{O}_B^i{}_j \equiv \begin{bmatrix} -(\partial_1^2 + \partial_2^2) \delta^i{}_j + \frac{\partial^2 \mathcal{W}}{\partial A_{\text{cl}}^i \partial A_{\text{cl}}^k} \frac{\partial^2 \mathcal{W}^*}{\partial A_{\text{cl}}^{*k} \partial A_{\text{cl}}^{*j}} & \frac{\partial^3 \mathcal{W}}{\partial A_{\text{cl}}^i \partial A_{\text{cl}}^k \partial A_{\text{cl}}^j} \frac{\partial \mathcal{W}^*}{\partial A_{\text{cl}}^{*k}} \\ \frac{\partial^3 \mathcal{W}^*}{\partial A_{\text{cl}}^{*i} \partial A_{\text{cl}}^{*k} \partial A_{\text{cl}}^{*j}} \frac{\partial \mathcal{W}}{\partial A_{\text{cl}}^k} & -(\partial_1^2 + \partial_2^2) \delta^i{}_j + \frac{\partial^2 \mathcal{W}^*}{\partial A_{\text{cl}}^{*i} \partial A_{\text{cl}}^{*k}} \frac{\partial^2 \mathcal{W}}{\partial A_{\text{cl}}^k \partial A_{\text{cl}}^j} \end{bmatrix} \quad (3.35)$$

$$\mathcal{O}_B^i{}_j \begin{bmatrix} A_n'^{*j} \\ A_n'^j \end{bmatrix} = M_n^2 \begin{bmatrix} A_n'^{*i} \\ A_n'^i \end{bmatrix}, \quad (3.36)$$

where the eigenvalue M_n^2 has to be real from Majorana condition. The quantum fluctuation for scalar can be expanded in terms of these mode functions to obtain a real scalar field equation with the mass M_n for the coefficient bosonic field $a_n(x^0, x^3)$

$$A^i(x^0, x^1, x^2, x^3) = \sum_n a_n(x^0, x^3) A_n^i(x^1, x^2) \quad (3.37)$$

$$(\partial_0^2 - \partial_3^2 + M_n^2) a_n(x^0, x^3) = 0. \quad (3.38)$$

Similarly the linearized equation for fermions is given by

$$-i\bar{\sigma}^\mu \partial_\mu \psi^i - \frac{\partial^2 \mathcal{W}^*}{\partial A_{\text{cl}}^{*i} \partial A_{\text{cl}}^{*j}} \bar{\psi}^j = 0 \quad (3.39)$$

$$-i\sigma^\mu\partial_\mu\bar{\psi}^i - \frac{\partial^2\mathcal{W}}{\partial A_{\text{cl}}^i\partial A_{\text{cl}}^j}\psi^j = 0. \quad (3.40)$$

To separate variables for fermion equations, it is more convenient to use a gamma matrix representation where direct product structure of 2×2 matrices for (x^0, x^3) and (x^1, x^2) space is manifest. We shall describe one such representation in appendix B. Transforming from such a representation to the Weyl representation which we are using, we can define the fermionic modes $\psi_{n\alpha}^i, \bar{\psi}_n^{i\dot{\beta}}$ combining components of left-handed and right-handed spinors by means of the following operators

$$\mathcal{O}_1^i{}_j \equiv \begin{bmatrix} -\frac{\partial^2\mathcal{W}^*}{\partial A_{\text{cl}}^{*i}\partial A_{\text{cl}}^{*j}} & -i(-\partial_1 + i\partial_2)\delta_j^i \\ -i(\partial_1 + i\partial_2)\delta_j^i & -\frac{\partial^2\mathcal{W}}{\partial A_{\text{cl}}^i\partial A_{\text{cl}}^j} \end{bmatrix} \quad (3.41)$$

$$\mathcal{O}_2^i{}_j \equiv \begin{bmatrix} -\frac{\partial^2\mathcal{W}}{\partial A_{\text{cl}}^i\partial A_{\text{cl}}^j} & -i(\partial_1 - i\partial_2)\delta_j^i \\ -i(-\partial_1 - i\partial_2)\delta_j^i & -\frac{\partial^2\mathcal{W}^*}{\partial A_{\text{cl}}^{*i}\partial A_{\text{cl}}^{*j}} \end{bmatrix} \quad (3.42)$$

$$\mathcal{O}_1^i{}_j \begin{bmatrix} \bar{\psi}_n^{j1} \\ \bar{\psi}_n^{j2} \end{bmatrix} = -im_n^{(1)} \begin{bmatrix} \psi_{n1}^i \\ \bar{\psi}_n^{i2} \end{bmatrix} \quad (3.43)$$

$$\mathcal{O}_2^i{}_j \begin{bmatrix} \psi_{n1}^j \\ \bar{\psi}_n^{j2} \end{bmatrix} = im_n^{(2)} \begin{bmatrix} \bar{\psi}_n^{i1} \\ \psi_{n2}^i \end{bmatrix}, \quad (3.44)$$

where the mass eigenvalues $m_n^{(1)}, m_n^{(2)}$ are real. Please note a peculiar combination of left- and right-handed spinor components to define eigenfunctions. We can expand ψ^i in terms of these mode functions

$$\psi_\alpha^i(x^0, x^1, x^2, x^3) = \sum_n \begin{pmatrix} b_n(x^0, x^3)\psi_{n1}^i(x^1, x^2) \\ c_n(x^0, x^3)\psi_{n2}^i(x^1, x^2) \end{pmatrix} \quad (3.45)$$

Since $\psi(x^0, x^1, x^2, x^3)$ is a Majorana spinor, the coefficient fermionic fields b_n, c_n are real. The linearized equations (3.39) (3.40) for the fermion gives a Dirac equation in $1+1$ dimensions for the coefficient fermionic fields (c_n, ib_n) with two mass parameters $m_n^{(1)}, m_n^{(2)}$

$$\left[-i(\rho_1\partial_0 + i\rho_2\partial_3) - m_n^{(1)}\frac{1+\rho_3}{2} - m_n^{(2)}\frac{1-\rho_3}{2} \right] \begin{bmatrix} c_n(x^0, x^3) \\ ib_n(x^0, x^3) \end{bmatrix} = 0, \quad (3.46)$$

where we use Pauli matrices ρ_a , $a = 1, 2, 3$ to construct the 2×2 gamma matrices $\rho_1, i\rho_2$ in $1+1$ dimensions. Since we have a Majorana spinor in $1+1$ dimensions which does not allow chiral rotations, we have two distinct real mass parameters $m_n^{(1)}, m_n^{(2)}$.

To relate the mass eigenvalues of fermions and bosons, let us multiply two differential operators for fermions \mathcal{O}_2 to \mathcal{O}_1 . In this ordering, we can use the BPS equation (2.16) corresponding to $H = H_{\text{II}}$ to find the differential operator for bosons \mathcal{O}_B

$$\mathcal{O}_{2k}^i\mathcal{O}_{1j}^k = \begin{bmatrix} e^{i\frac{\pi}{4}}\Omega_-^{\frac{1}{2}} & 0 \\ 0 & e^{-i\frac{\pi}{4}}\Omega_-^{-\frac{1}{2}} \end{bmatrix} \mathcal{O}_{Bj}^i \begin{bmatrix} e^{-i\frac{\pi}{4}}\Omega_-^{-\frac{1}{2}} & 0 \\ 0 & e^{i\frac{\pi}{4}}\Omega_-^{\frac{1}{2}} \end{bmatrix}. \quad (3.47)$$

Therefore the BPS equation (2.16) corresponding to $H = H_{\text{II}}$ guarantees that the existence of a solution $\bar{\psi}_n^{i1}, \psi_{n2}^i$ of fermionic mode equations implies the existence of a solution of bosonic mode equations with the mass squared $M_n^2 = m_n^{(1)} m_n^{(2)}$

$$A_n'^{*i} = e^{-i\frac{\pi}{4}} \Omega_-^{-\frac{1}{2}} \bar{\psi}_n^{i1}, \quad A_n^i = e^{i\frac{\pi}{4}} \Omega_-^{\frac{1}{2}} \psi_{n2}^i. \quad (3.48)$$

If another BPS equation (2.13) corresponding to $H = H_{\text{I}}$ is valid, operator multiplication with different ordering gives the same bosonic operator whose rows and columns are interchanged

$$\mathcal{O}_{1k}^i \mathcal{O}_{2j}^k = \begin{bmatrix} 0 & e^{i\frac{\pi}{4}} \Omega_+^{-\frac{1}{2}} \\ -e^{-i\frac{\pi}{4}} \Omega_+^{\frac{1}{2}} & 0 \end{bmatrix} \mathcal{O}_{Bj}^i \begin{bmatrix} 0 & -e^{i\frac{\pi}{4}} \Omega_+^{-\frac{1}{2}} \\ e^{-i\frac{\pi}{4}} \Omega_+^{\frac{1}{2}} & 0 \end{bmatrix}. \quad (3.49)$$

Therefore the BPS equation (2.13) corresponding to $H = H_{\text{I}}$ guarantees that the existence of a solution $\bar{\psi}_n^{i2}, \psi_{n1}^i$ of fermionic mode equations implies the existence of a solution of bosonic mode equations with the mass squared $M_n^2 = m_n^{(1)} m_n^{(2)}$

$$A_n'^{*i} = -e^{i\frac{\pi}{4}} \Omega_+^{-\frac{1}{2}} \bar{\psi}_n^{i2}, \quad A_n^i = e^{-i\frac{\pi}{4}} \Omega_+^{\frac{1}{2}} \psi_{n1}^i. \quad (3.50)$$

Therefore we find that all massive states come in pairs of boson and fermion with the same mass squared $M_n^2 = m_n^{(1)} m_n^{(2)}$ in accordance with the result of the unitary representation of the $(1, 0)$ supersymmetry algebra.

3.2 Nambu-Goldstone modes

Since we are usually most interested in a low energy effective field theory, we wish to study massless modes here. If global continuous symmetries are broken spontaneously, there occur associated massless modes which are called the Nambu-Goldstone modes. To find the wave functions of the Nambu-Goldstone modes, we perform the associated global transformations and evaluate the transformed configuration by substituting the classical field. For supersymmetry we obtain nontrivial wave function by substituting the classical field $A_{\text{cl}}^i(x^1, x^2)$ and $F_{\text{cl}}^i(x^1, x^2)$ to the transformation of fermions by a Grassmann parameter ξ , since classical field configuration of fermion vanishes $\psi_{\text{cl}}^i = 0$

$$\delta_\xi \psi^i = i\sqrt{2} \sigma^\mu \bar{\xi} \partial_\mu A_{\text{cl}}^i + \sqrt{2} \xi F_{\text{cl}}^i. \quad (3.51)$$

If the BPS equation (2.16) for the junction background is valid, we obtain

$$\delta_\xi \psi^i = \sqrt{2} [(i\sigma^1 \bar{\xi} - \Omega_-^* \xi) \partial_1 A_{\text{cl}}^i + (i\sigma^2 \bar{\xi} + i\Omega_-^* \xi) \partial_2 A_{\text{cl}}^i]. \quad (3.52)$$

We see that there is one conserved direction in the Grassmann parameter:

$$i\sigma^1 \bar{\xi} = \Omega_-^* \xi \text{ and } \sigma^2 \bar{\xi} = -\Omega_-^* \xi. \quad (3.53)$$

The other three real Grassmann parameters ξ correspond to broken supercharges. For our exact solution, for instance, we find it convenient to choose the three broken supercharges as the following real supercharges

$$Q_I = \frac{1}{\sqrt{2}}(e^{i\pi/4}Q_2 + e^{-i\pi/4}\bar{Q}_{\dot{2}}), \quad Q_{II} = \frac{1}{\sqrt{2}}(e^{-i\pi/4}Q_1 + e^{i\pi/4}\bar{Q}_{\dot{1}}), \quad Q_{III} = \frac{1}{\sqrt{2}}(e^{i\pi/4}Q_1 + e^{-i\pi/4}\bar{Q}_{\dot{1}}). \quad (3.54)$$

Then the corresponding massless mode functions are given by

$$\psi_0^{(I)i}(x^1, x^2) = \begin{pmatrix} 4\partial_z A_{cl}^i(x^1, x^2)e^{-i\pi/4} \\ 0 \end{pmatrix}, \quad (3.55)$$

$$\psi_0^{(II)i}(x^1, x^2) = \begin{pmatrix} 0 \\ 2\partial_1 A_{cl}^i(x^1, x^2)e^{i\pi/4} \end{pmatrix}, \quad (3.56)$$

$$\psi_0^{(III)i}(x^1, x^2) = \begin{pmatrix} 0 \\ 2\partial_2 A_{cl}^i(x^1, x^2)e^{i\pi/4} \end{pmatrix}. \quad (3.57)$$

Since the transformation parameter should correspond to the Nambu-Goldstone field with zero momentum and energy, the three transformation parameters ξ should be promoted to three real fermionic fields in x^0, x^3 space, $b_0^{(I)}(x^0, x^3)$, $c_0^{(II)}(x^0, x^3)$, and $c_0^{(III)}(x^0, x^3)$, to obtain the Nambu-Goldstone component of the mode expansion

$$\begin{aligned} \psi^i(x^0, x^1, x^2, x^3) = & b_0^{(I)}(x^0, x^3)\psi_0^{(I)i}(x^1, x^2) + c_0^{(II)}(x^0, x^3)\psi_0^{(II)i}(x^1, x^2) \\ & + c_0^{(III)}(x^0, x^3)\psi_0^{(III)i}(x^1, x^2) + \sum_{n>0} \begin{pmatrix} b_n(x^0, x^3)\psi_{n1}^i(x^1, x^2) \\ c_n(x^0, x^3)\psi_{n2}^i(x^1, x^2) \end{pmatrix}. \end{aligned} \quad (3.58)$$

We have explicitly displayed three massless Nambu-Goldstone fermion components distinguishing from the massive ones ($n > 0$). The Dirac equation for the coefficient fermionic fields (3.46) shows that $b_0^{(I)}(x^0 - x^3)$ is a right-moving massless mode, and $c_0^{(II)}(x^0 + x^3)$, and $c_0^{(III)}(x^0 + x^3)$ are left-moving modes.

We plot the absolute values of $|\psi_0^{(a)i=T}|$ of the $i = T$ component of the wave function of the Nambu-Goldstone fermions $a = I, II, III$ in Fig. 2. We can see that Nambu-Goldstone fermions have wave functions which extend to infinity along three walls. They become identical to fermion zero modes on at least two of the walls asymptotically and hence they are not localized around the center of the junction. We can construct a linear combination of the Nambu-Goldstone fermions to have no support along one out of the three walls. However, no linear combination of these Nambu-Goldstone fermions can be formed which does not have support extended along any of the wall. Therefore these wave functions are not localized and are not normalizable. This fact means that the low energy dynamics of BPS junction cannot be described by a 1 + 1 dimensional effective field theory with a discrete particle spectrum.

Similarly the Nambu-Goldstone bosons corresponding to the broken translation $P^a, a = 1, 2$ are given by

$$A_0^{(a)}(x^1, x^2) = \partial_a A_{cl}^i(x^1, x^2), \quad a = 1, 2. \quad (3.59)$$

These two bosonic massless modes consist of two left-moving modes and two right-moving modes. On the other hand, we have seen already that there are two left-moving massless Nambu-Goldstone fermions and one right-moving massless Nambu-Goldstone fermion. These two left-moving Nambu-Goldstone bosons and fermions form two doublets of the $(1, 0)$ supersymmetry algebra. The right-moving modes are asymmetric in bosons and fermions: two Nambu-Goldstone bosons and a single Nambu-Goldstone fermion. These three states are all singlets of the $(1, 0)$ supersymmetry algebra in accordance with our analysis in sect.2.3. Therefore we obtained a chiral structure of Nambu-Goldstone fermions on the junction background configuration.

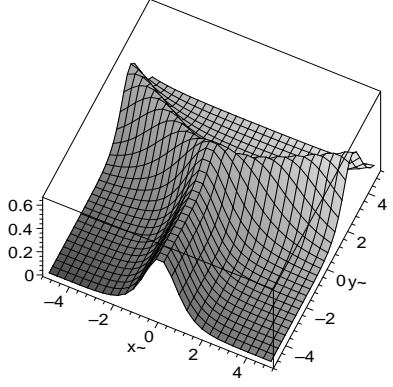
3.3 Non-normalizability of the Nambu-Goldstone fermions

We would like to argue that our observation is a generic feature of the Nambu-Goldstone fermions on the domain wall junction in a flat space in the bulk: Nambu-Goldstone fermions are not localized at the junction and hence are not normalizable, if they are associated with the supersymmetry breaking due to the coexistence of nonparallel domain walls. The following observation is behind this assertion. A single domain wall breaks only a half of supercharges. Nonparallel wall also breaks half of supercharges, some of which may be linear combinations of the supercharges already broken by the first wall. If the junction configuration is a $1/4$ BPS state, linearly independent ones among these two sets of broken supercharges of nonparallel walls become $\frac{3}{4}$ of the original supercharges.

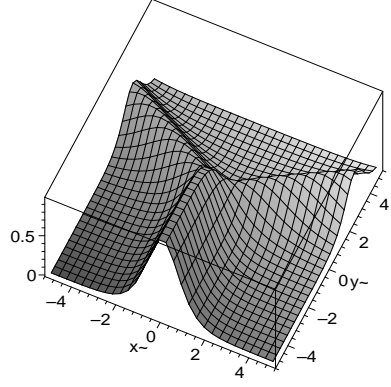
To see in more detail, let us first note that the junction configuration reduces asymptotically to a wall if one goes along the wall, say the wall 1. On this first wall, a half of the original supersymmetry $(Q^{(1)}, \dots, Q^{(N)})$ is broken. Denoting the number of original supercharges to be N , we call these broken supercharges as $Q^{(1)}, \dots, Q^{(N/2)}$. Consequently we have Nambu-Goldstone fermions localized around the core of the wall and is constant along the wall. In the junction configuration, we have other walls which are not parallel to the first wall. Asymptotically far away along one of such walls, say wall 2, another half of the supersymmetry $Q'^{(1)}, \dots, Q'^{(N/2)}$ is broken. If the junction is a $1/4$ BPS state, a half of these, say $Q'^{(1)}, \dots, Q'^{(N/4)}$, is a linear combination of $Q^{(1)}, \dots, Q^{(N/2)}$ broken already on the wall 1. The other half, $Q'^{(N/4+1)}, \dots, Q'^{(N/2)}$ are unbroken on the wall 1. Altogether a quarter of the original supercharges remain unbroken. Consequently the Nambu-Goldstone fermions corresponding to $Q'^{(1)}, \dots, Q'^{(N/4)}$ have a wave function which extends to infinity and approaches a constant profile along both the walls 1 and 2. Those modes corresponding to $Q'^{(N/4+1)}, \dots, Q'^{(N/2)}$ have support only along the wall 2, and those corresponding to the linear combinations of $Q^{(1)}, \dots, Q^{(N/2)}$ orthogonal to $Q'^{(1)}, \dots, Q'^{(N/4)}$ have support only along the wall 1. Thus we find that any linear combinations of the Nambu-Goldstone fermions have to be infinitely extended along at least one of the walls which form the junction configuration. Therefore the Nambu-Goldstone fermions associated with the coexistence of nonparallel domain walls are not localized at the junction and are not normalizable.

In our exact solution, domain wall junction configuration reduces asymptotically to the wall 1 at $x^2 \rightarrow -\infty$ with fixed x^1 . On the wall, only two supercharges in Eq.(3.54) are broken

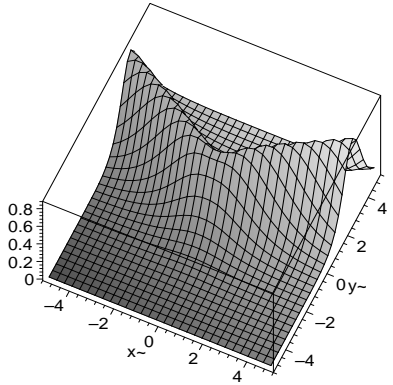
$$Q_I = \frac{1}{\sqrt{2}}(e^{i\pi/4}Q_2 + e^{-i\pi/4}\overline{Q}_2), \quad Q_{II} = \frac{1}{\sqrt{2}}(e^{-i\pi/4}Q_1 + e^{i\pi/4}\overline{Q}_1), \quad (3.60)$$



The wave function $\left| \psi_0^{(I)T} \right|$



The wave function $\left| \psi_0^{(II)T} \right|$



The wave function $\left| \psi_0^{(III)T} \right|$

Figure 2: The bird's eye view of the absolute value of the $i = T$ component of the wave functions of the Nambu-Goldstone fermions on the junction in the (x^1, x^2) space

and there are two corresponding Nambu-Goldstone fermions which become domain wall zero modes asymptotically

$$\begin{aligned}\psi_0^{(\text{I})i}(x^1, x^2) &= \begin{pmatrix} 4\partial_z A_{\text{cl}}^i(x^1, x^2)e^{-i\pi/4} \\ 0 \end{pmatrix} \rightarrow \begin{pmatrix} 2\partial_1 A_{\text{cl}}^{i\text{wall}}(x^1)e^{-i\pi/4} \\ 0 \end{pmatrix}, \\ \psi_0^{(\text{II})i}(x^1, x^2) &= \begin{pmatrix} 0 \\ 2\partial_1 A_{\text{cl}}^i(x^1, x^2)e^{i\pi/4} \end{pmatrix} \rightarrow \begin{pmatrix} 0 \\ 2\partial_1 A_{\text{cl}}^{i\text{wall}}(x^1)e^{i\pi/4} \end{pmatrix}.\end{aligned}\quad (3.61)$$

These wave functions are localized on the core of the wall 1 in the x^1 direction and are constant along the wall. Along the other walls we find two broken supercharges one of which is identical to one of the broken supercharges, Q_{I} . The other broken supercharge is Q'_{II} on the wall 2 and Q''_{II} on the wall 3. There are only two independent supercharges among Q_{II} , Q'_{II} , and Q''_{II} . Together with Q_{I} we obtain three independent broken supercharges. We can construct a linear combination of the Nambu-Goldstone fermions to have no support along one out of the three walls. However, any linear combination has nonvanishing wave function which becomes fermion zero mode on at least one of the wall asymptotically. Therefore the associated Nambu-Goldstone fermions have support which is infinitely extended at least along two of the walls.

If a single wall is present, we can explicitly construct a plane wave solution propagating along the wall, which may be called a spin wave and is among massive modes on the wall background. Even if there are several walls forming a junction configuration, we can consider excitation modes which reduce to the spin wave modes along each wall. They should be a massive mode on the domain wall junction background. The Nambu-Goldstone mode on the domain wall junction is the zero wave number limit of such a spin wave mode. This physical consideration suggests that the massless Nambu-Goldstone fermion is precisely the vanishing wave number (along the wall) limit of the massive spin wave mode.

Let us note that our argument does not apply to models with the bulk cosmological constant. In such models, massless graviton is localized on the background of intersection of walls [3]. In that case, massless mode is a distinct mode different from the massless limit of the massive continuum, although the massless mode is buried at the tip of the continuum of massive modes. The normalizability of the massless graviton is guaranteed by the Anti de Sitter geometry away from the junction or intersection including the direction along the wall.

4 Boundary conditions and central charges

For a 1/4 BPS state, there are two sets of BPS equations, Eqs.(2.13)–(2.15) and (2.16)–(2.17), corresponding to the two kinds of BPS domain wall junctions. In this section we make explicit the relation between the boundary conditions and the choice of these BPS equations.

BPS domain wall junction is formed when nonparallel BPS walls meet at a junction. In regions far away from the junction, the configuration approaches to isolated walls asymptotically. BPS domain wall is a 1/2 BPS state and conserves two supercharges. These two supercharges are given, from Eqs.(2.11) and (2.12), in terms of central charges Z_1 and Z_2 for the wall. Let us take a general Wess-Zumino model in Eq.(2.3) and examine if a domain wall junction can be formed

where N different vacua appear in asymptotic regions. These N vacua correspond to N points in the complex plane of superpotential \mathcal{W} . The field configuration of the junction at infinity is mapped to a straight line connecting these N vertices [14], [16]. In order to have a balance of force, this polygon has to be convex [14]. We set the origin of the \mathcal{W} space at an arbitrary point inside this BPS polygon and denote the value of the superpotential at the I -th vacuum as \mathcal{W}_I , for $I = 1, \dots, N$, as illustrated in Fig. 3(b). Let us take the origin in x^1, x^2 space as the junction point of these BPS walls. If we denote θ_{IJ} the angle of the half wall separating two vacua, I and J , as illustrated in Fig. 3(a), the central charges Z_1 and Z_2 of this wall are given by Eq.(2.4) as

$$\vec{Z}_{IJ} \equiv (Z_1, Z_2)_{IJ} = 2 [\mathcal{W}_J^* - \mathcal{W}_I^*] \cdot \vec{\omega}_{IJ} \cdot (\text{Area}), \quad (4.62)$$

$$\vec{\omega}_{IJ} \equiv (\cos(\theta_{IJ} + \pi/2), \sin(\theta_{IJ} + \pi/2)). \quad (4.63)$$

Thus two supercharges conserved at this wall are

$$Q_1 + e^{i(-\alpha_{IJ} - \theta_{IJ})} \bar{Q}_1, \quad Q_2 + e^{i(-\alpha_{IJ} + \theta_{IJ})} \bar{Q}_2, \quad (4.64)$$

where $\alpha_{IJ} = \arg(\mathcal{W}_J - \mathcal{W}_I)$.

BPS domain wall junction is a $1/4$ BPS state and conserves only one supercharge. Let us consider the case of $H = H_{\text{II}}$ where a linear combination of Q_2 and \bar{Q}_2 is conserved as shown in Eq.(2.12). This must be the common conserved supercharge for all the walls

$$\dots = Q_2 + e^{i(-\alpha_{IJ} + \theta_{IJ})} \bar{Q}_2 = Q_2 + e^{i(-\alpha_{JK} + \theta_{JK})} \bar{Q}_2 = \dots \quad (4.65)$$

Then the relative angle of the two neighboring walls must be equal to the difference of two phases of the differences $\Delta\mathcal{W}$ of the superpotentials for the two walls

$$\dots, \theta_{JK} - \theta_{IJ} = \alpha_{JK} - \alpha_{IJ}, \dots \quad (4.66)$$

Moreover the field configuration at infinity should move counterclockwise in \mathcal{W} space, as we go around the origin counterclockwise in x^1, x^2 space.

Similarly, a linear combination of Q_1 and \bar{Q}_1 is the common conserved supercharge in the case of $H = H_{\text{I}}$. We obtain in this case

$$\dots, \theta_{JK} - \theta_{IJ} = -(\alpha_{JK} - \alpha_{IJ}), \dots \quad (4.67)$$

and that the field configuration at infinity should move clockwise in \mathcal{W} space, as we go around the origin counterclockwise in x^1, x^2 space.

Therefore we find that the BPS equations (2.16)–(2.17) for the case $H = H_{\text{II}}$ should be used if the phase of the superpotential \mathcal{W} increases as we go around the origin counterclockwise in x^1, x^2 space. If the phase of the superpotential \mathcal{W} decreases as we go around the origin counterclockwise in x^1, x^2 space, the other BPS equations (2.13)–(2.15) for $H = H_{\text{I}}$ should be used.

Next we discuss the sign of the contribution of the central charge Y_3 to the mass of the junction configuration. We can use the Stokes theorem to obtain an expression for the central charge Y_3 as a contour integral [17] [14]

$$Y_3 = \int dx^3 i \int d^2x [\partial_1 (K_i \partial_2 A^i) - \partial_2 (K_i \partial_1 A^i)] = \int dx^3 i \oint K_i dA^i, \quad (4.68)$$

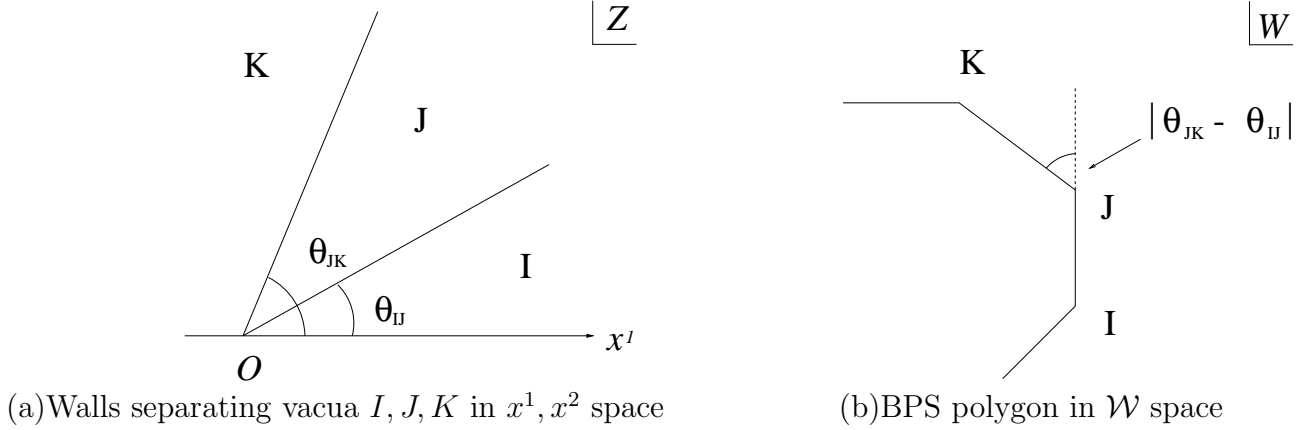


Figure 3: Walls in x^1, x^2 space and BPS polygon in W space

where $K_i \equiv \partial K / \partial A^i$ is a derivative of the Kähler potential K . This contour integral in the field space should be done as a map from a counterclockwise contour in the infinity of $z = x^1 + ix^2$ plane. Only complex fields can contribute to Y_3 . Let us assume for simplicity that there is only one field which can contribute to Y_3 as in our exact solution.

Eq.(4.68) shows that the central charge Y_3 becomes negative (positive), if the asymptotic counterclockwise contour in x^1, x^2 is mapped into a counterclockwise (clockwise) contour in field space. On the other hand, the sign of the contribution of the central charge Y_3 to the mass of the junction configuration is determined by the formula $H = H_{II} = |\langle iZ_1 - Z_2 \rangle| + \langle Y_3 \rangle$, or $H = H_I = |\langle -iZ_1 - Z_2 \rangle| - \langle Y_3 \rangle$. The choice of these mass formulas are in turn determined by the map of the asymptotic counterclockwise contour in x^1, x^2 space to a counterclockwise or clockwise contour in the superpotential space W . Combining these two observations, we conclude that the contribution of the central charge Y_3 to the mass of the junction configuration is negative if the sign of rotations is the same in field space A^i and in superpotential space W , and positive if the sign of rotations is opposite.

The field configuration moves counterclockwise in field space in our exact solution in (2.24) and then the central charge is negative in this solution. Since the exact solution satisfies the BPS equation for the case $H = H_{II}$, the central charge contributes to the mass of the junction configuration negatively. Therefore we should not consider the central charge Y_3 alone as the physical mass of the junction at the center. In the junction configuration, the junction at the center cannot be separated from the walls. We also can find a solution for the other case of $H = H_I$ in our model. The solution is just a configuration obtained by a reflection $x^1 \rightarrow -x^1$. Then the central charge is positive, but the contribution to the mass $H = H_I$ becomes again negative. In either solution, the rotation in field T space has the same sign as the rotation in superpotential W space. Therefore central charge Y_3 contributes negatively to the mass of the junction, irrespective of the choice of $H = H_I$ or $H = H_{II}$.

More recently this feature of negative contribution of Y_3 to the junction mass is studied from a different viewpoint and it is argued that this feature is valid in most situations except possibly in contrived models [22]. These models, if they exist, should correspond to the case of opposite sign of rotations in \mathcal{W} space and field space.

5 Energy density and central charges

5.1 Charge densities

Our exact solution is useful to examine how the topological charges Z_k , Y_k and energy of the domain wall junction are distributed in x^1, x^2 space. We shall study their densities and integrated quantities in finite regions in this section.

5.1.1 Y charge density

The Y_3 charge density $\mathcal{Y}_3 = i\epsilon^{3nm}\partial_n(T^*\partial_m T)$ is given in our exact solution by

$$\begin{aligned}\mathcal{Y}_3 &= -24\Lambda^4 \frac{e^{\sqrt{3}\Lambda x^2}}{\left[e^{\sqrt{3}\Lambda x^2} + 2\cosh(\Lambda x^1)\right]^3} \\ &= -24\Lambda^4 \frac{1}{\left[e^{\frac{2\Lambda r}{\sqrt{3}}\sin\theta} + e^{\frac{2\Lambda r}{\sqrt{3}}\sin(\theta+\frac{2\pi}{3})} + e^{\frac{2\Lambda r}{\sqrt{3}}\sin(\theta-\frac{2\pi}{3})}\right]^3}\end{aligned}\quad (5.69)$$

where the cylindrical coordinates r and θ is used to make Z_3 symmetry explicit. A bird's eye view of the \mathcal{Y}_3 is given in Fig. 4. Here and the following, we shall take the unit of $\Lambda \equiv 1$ in drawing figures. The density is localized near the origin and the Z_3 symmetry is manifest.

5.1.2 Z charge density

We obtain the superpotential as the function of x^1 and x^2 , by inserting the solution (2.24)

$$\begin{aligned}\text{Re}\mathcal{W}^* &= -8\Lambda^3 \frac{\left(2 + 3e^{\sqrt{3}\Lambda x^2}\cosh(\Lambda x^1) + \cosh(2\Lambda x^1)\right)\sinh(\Lambda x^1)}{\left[e^{\sqrt{3}\Lambda x^2} + 2\cosh(\Lambda x^1)\right]^3} \\ \text{Im}\mathcal{W}^* &= 2\sqrt{3}\Lambda^3 \frac{e^{\sqrt{3}\Lambda x^2}\left[2 + e^{2\sqrt{3}\Lambda x^2} + 6e^{\sqrt{3}\Lambda x^2}\cosh(\Lambda x^1)\right]}{\left[e^{\sqrt{3}\Lambda x^2} + 2\cosh(\Lambda x^1)\right]^3}.\end{aligned}\quad (5.70)$$

The Z charge densities are given by $\mathcal{Z}_k = 2\partial_k\mathcal{W}^*$, ($k = 1, 2$) and are found to be

$$\text{Re}\mathcal{Z}_1 = -48\Lambda^4 \frac{2 + e^{2\sqrt{3}\Lambda x^2}\cosh(2\Lambda x^1) + 3e^{\sqrt{3}\Lambda x^2}\cosh(\Lambda x^1)}{\left[e^{\sqrt{3}\Lambda x^2} + 2\cosh(\Lambda x^1)\right]^4}$$

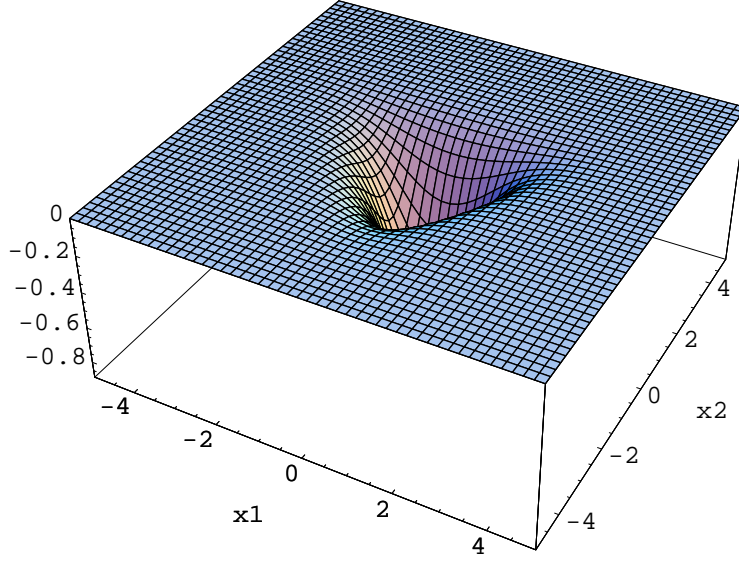


Figure 4: A bird's eye view of \mathcal{Y}_3 .

$$\begin{aligned}
\text{Im}\mathcal{Z}_1 &= -\text{Re}\mathcal{Z}_2 = -48\sqrt{3}\Lambda^4 \frac{e^{\sqrt{3}\Lambda x^2} \sinh(\Lambda x^1) \left(1 + 2e^{\sqrt{3}\Lambda x^2} \cosh(\Lambda x^1)\right)}{\left[e^{\sqrt{3}\Lambda x^2} + 2 \cosh(\Lambda x^1)\right]^4} \\
\text{Im}\mathcal{Z}_2 &= 48\Lambda^4 \frac{e^{\sqrt{3}\Lambda x^2} \left[\cosh(\Lambda x^1) + e^{\sqrt{3}\Lambda x^2} (2 + 3 \cosh(2\Lambda x^1))\right]}{\left[e^{\sqrt{3}\Lambda x^2} + 2 \cosh(\Lambda x^1)\right]^4}.
\end{aligned} \tag{5.71}$$

We can define the effective value of the Z charge which contributes to the energy of the junction as $Z_{\text{eff}} = -\text{Re}\mathcal{Z}_1 + \text{Im}\mathcal{Z}_2$. Corresponding effective charge density is given by

$$\mathcal{Z}_{\text{eff}} = 96\Lambda^4 \frac{1 + 2e^{\sqrt{3}\Lambda x^2} \cosh(\Lambda x^1) + e^{2\sqrt{3}\Lambda x^2} (1 + 2 \cosh(2\Lambda x^1))}{\left[e^{\sqrt{3}\Lambda x^2} + 2 \cosh(\Lambda x^1)\right]^4}. \tag{5.72}$$

Let us note that the effective charge density is Z_3 symmetric, whereas individual charges $\mathcal{Z}_1, \mathcal{Z}_2$ are not.

5.1.3 Energy density

Adding \mathcal{Z}_{eff} and \mathcal{Y}_3 together, the energy density of the junction is obtained,

$$\mathcal{H} = 24\Lambda^4 \frac{4 + 6e^{\sqrt{3}\Lambda x^2} \cosh(\Lambda x^1) + e^{2\sqrt{3}\Lambda x^2} (3 + 8 \cosh(2\Lambda x^1))}{\left[e^{\sqrt{3}\Lambda x^2} + 2 \cosh(\Lambda x^1)\right]^4} \tag{5.73}$$

A bird's eye view of \mathcal{H} is shown in Fig. 5. The energy density is Z_3 symmetric as expected.

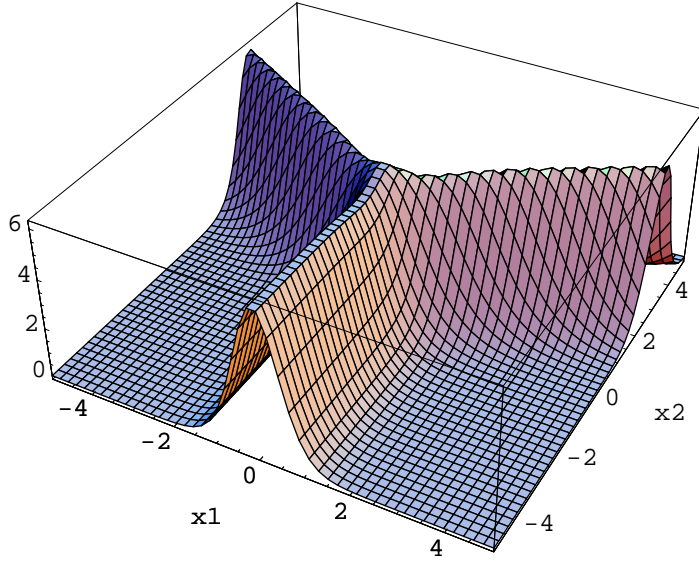


Figure 5: A bird's eye view of the energy density of the junction.

A cross section of the densities, \mathcal{H} , \mathcal{Z}_{eff} and \mathcal{Y}_3 along one of the walls (e.g. negative x^2 direction) is shown in Fig. 6. The \mathcal{Z}_{eff} charge contributes to the energy positively while \mathcal{Y}_3 does negatively. Since the decrease of \mathcal{Z}_{eff} is faster than the increase of \mathcal{Y}_3 , a small dip is found around $R\Lambda \sim 1$. Far from the origin there is practically no difference between \mathcal{Z}_{eff} and \mathcal{H} because \mathcal{Y}_3 is localized near the origin.

5.2 Charge densities integrated over a region of finite radius

In this subsection we shall evaluate the central charge densities integrated over a triangular or circular region depicted in Fig. 7.

5.2.1 \mathcal{Y}_3 charge

Integrating \mathcal{Y}_3 over a triangle whose inscribed circle has a radius R as shown in Fig. 7, we obtain for large R ($R\Lambda \gg 1$)

$$Y_3^{\text{triangle}}(R) = -2\sqrt{3}\Lambda^2 L_3 \left[1 - \frac{3\pi}{4} e^{-\sqrt{3}R\Lambda} + \mathcal{O}\left(e^{-2\sqrt{3}R\Lambda}\right) \right], \quad (5.74)$$

where L_3 denotes the length along the x^3 direction. The leading term agrees with our previous evaluation by the step function approximation[17] and the subleading terms vanish exponentially as $R \rightarrow \infty$.

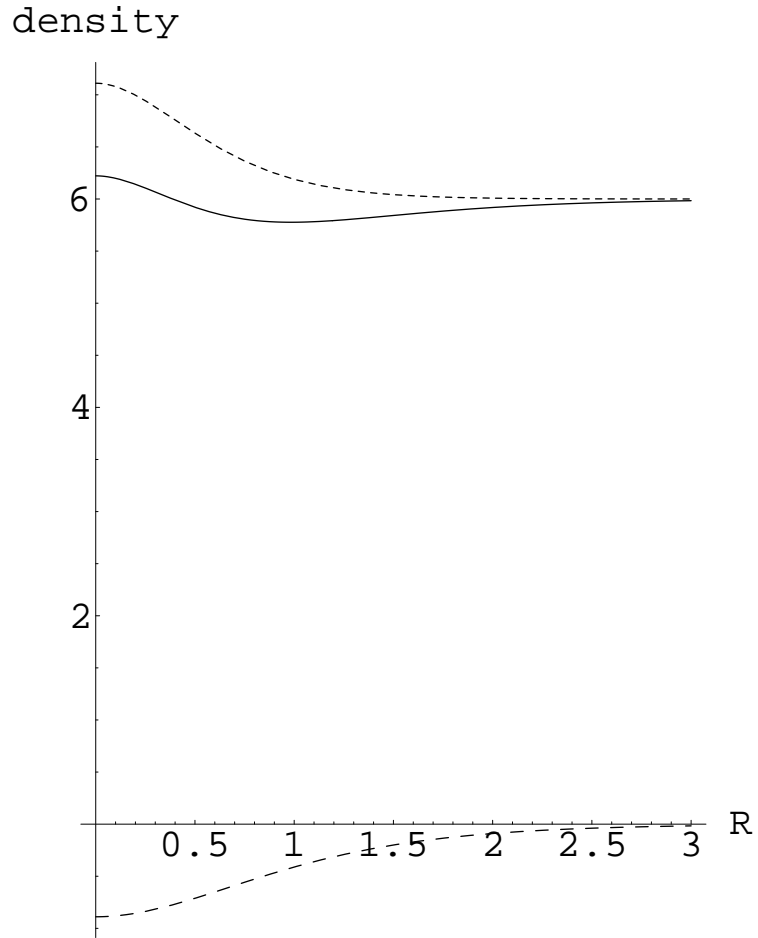


Figure 6: A cross section of the densities \mathcal{H} (solid line), \mathcal{Z}_{eff} (short dashed line) and \mathcal{Y}_3 (long dashed line) along the negative x^2 direction.

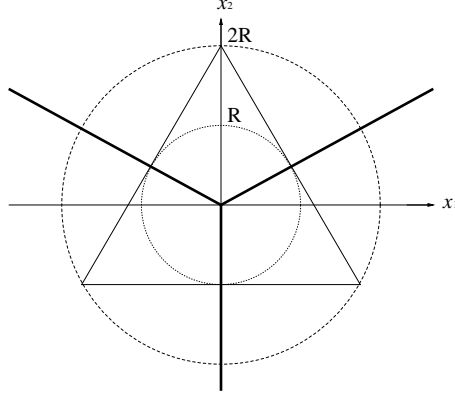


Figure 7: The domains of integration: triangle (solid line), inscribed circle (short dashed line) and circumscribed circle (long dashed line). The bold lines denote the domain walls forming a junction.

On the other hand, for small R ($R\Lambda \ll 1$), we obtain the Y_3 charge

$$Y_3^{\text{triangle}}(R) = -\frac{8}{\sqrt{3}}\Lambda^2 L_3 \left[R^2 \Lambda^2 - R^4 \Lambda^4 - \frac{4\sqrt{3}}{45} R^5 \Lambda^5 + \mathcal{O}(R^6 \Lambda^6) \right]. \quad (5.75)$$

Notice that the leading term comes from the density at the origin multiplied by the area of the circle. Although there are no terms of the first or third degree in R , there is a fifth degree term.

We can also integrate the \mathcal{Y}_3 over a circle of radius R . In this case it is more convenient to use cylindrical coordinates $(r, \theta, \text{ and } x^3)$, and the following surface integral formula obtained from the Stokes theorem,

$$\begin{aligned} Y_3^{\text{circle}}(R) &= \int_{-L_3/2}^{L_3/2} dx^3 \int_0^{2\pi} d\theta \left[iT'^* \frac{\partial}{\partial \theta} T' \right] \\ &= \frac{8R\Lambda^3 L_3}{\sqrt{3}} \int_0^{2\pi} d\theta \frac{\sin\left(\theta - \frac{2\pi}{3}\right) e^{2R\Lambda \cos \theta} + \sin \theta e^{2R\Lambda \cos\left(\theta + \frac{2\pi}{3}\right)} + \sin\left(\theta + \frac{2\pi}{3}\right) e^{2R\Lambda \cos\left(\theta - \frac{2\pi}{3}\right)}}{\left[e^{\frac{2R\Lambda}{\sqrt{3}} \sin\left(\theta + \frac{2\pi}{3}\right)} + e^{\frac{2R\Lambda}{\sqrt{3}} \sin\left(\theta - \frac{2\pi}{3}\right)} + e^{\frac{2R\Lambda}{\sqrt{3}} \sin \theta} \right]^3} \end{aligned} \quad (5.76)$$

where the Z_3 symmetry is manifest. Expanding the integrand for small R ($R\Lambda \ll 1$), we obtain

$$Y_3^{\text{circle}}(R) = -\frac{8\pi}{9}\Lambda^2 L_3 \left[R^2 \Lambda^2 - \frac{1}{2} R^4 \Lambda^4 + \mathcal{O}(R^6 \Lambda^6) \right]. \quad (5.77)$$

The leading term is again the density at the origin multiplied by the area of the circle. In contrast to the triangle case, there is no term of odd degree in R .

For large R ($R\Lambda \gg 1$), we have to perform numerical integration to evaluate the $Y_3^{\text{circle}}(R)$. We compare the $Y_3(R)$ evaluated for triangle, inscribed and circumscribed circle in Fig. 8. In the limit of $R \rightarrow \infty$, $Y_3(R)$ for all the regions converge to $-2\sqrt{3}\Lambda^2 L_3$ as expected.

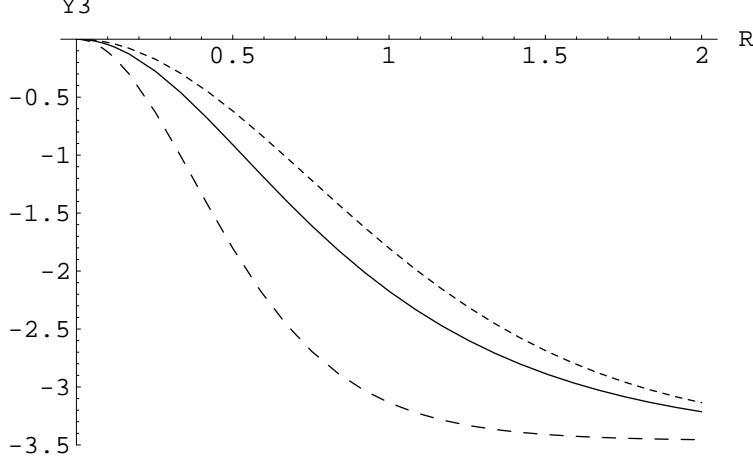


Figure 8: $Y_3(R)$ evaluated for the triangle (solid line), inscribed circle of radius R (short dashed line) and circumscribed circle (long dashed line).

5.2.2 Z charges

Since the Z_1 charge is given by a total derivative in x^1 , we can rewrite the Z_1 charge as

$$Z_1(R) = 2 \int dx^2 \int dx^1 \partial_1 \mathcal{W}^*(A^*) = 2 \int_{x^{2-}}^{x^{2+}} dx^2 [\mathcal{W}^*(x^{1+}(x^2), x^2) - \mathcal{W}^*(x^{1-}(x^2), x^2)], \quad (5.78)$$

where $x^{i\pm}$ ($i = 1, 2$) denote the upper and lower bound of the domain of integration. Since Eq.(5.70) shows that $\text{Im}\mathcal{W}^*(x^1, x^2)$ is even and $\text{Re}\mathcal{W}^*(x^1, x^2)$ is odd in x^1 , we obtain $\text{Im}Z_1(R) = 0$ and $\text{Re}Z_2(R) = 0$ for an integration region symmetric in x^1 which we shall use. Let us note that $\text{Re}Z_1$ ($\text{Im}Z_2$) is negative (positive) definite.

Firstly we choose as a domain of integration the triangle region whose inscribed circle has a radius R . For large R ($R\Lambda \gg 1$), we obtain

$$\begin{aligned} \text{Re}Z_1^{\text{triangle}}(R) &= -12\Lambda^2 L_3 \left[R\Lambda + \frac{\sqrt{3}\pi}{4} e^{-\sqrt{3}R\Lambda} + \mathcal{O}(e^{-2\sqrt{3}R\Lambda}) \right] \\ \text{Im}Z_2^{\text{triangle}}(R) &= 12\Lambda^2 L_3 \left[R\Lambda + \frac{\sqrt{3}}{3} \left(\frac{\pi}{8} - \frac{4}{3} \right) e^{-\sqrt{3}R\Lambda} + \mathcal{O}(e^{-2\sqrt{3}R\Lambda}) \right]. \end{aligned} \quad (5.79)$$

The leading linear term represents the contribution of charge density per unit length of the wall. It is interesting to observe that there are no constant terms. The exponentially suppressed terms represent the way the domain wall junction configuration converges to isolated walls as $R \rightarrow \infty$. The effective value of the Z charge becomes

$$\begin{aligned} Z_{\text{eff}}^{\text{triangle}}(R) &= -\text{Re}Z_1^{\text{triangle}}(R) + \text{Im}Z_2^{\text{triangle}}(R) \\ &= 24\Lambda^3 L_3 R + \sqrt{3} \left(\frac{7\pi}{2} - \frac{16}{3} \right) \Lambda^2 L_3 e^{-\sqrt{3}R\Lambda} + \mathcal{O}(e^{-2\sqrt{3}R\Lambda}). \end{aligned} \quad (5.80)$$

For small R ($R\Lambda \ll 1$), Z charges become

$$\begin{aligned}\text{Re}Z_1^{\text{triangle}}(R) &= -\frac{32}{\sqrt{3}}\Lambda^2 L_3 \left[R^2\Lambda^2 + \frac{1}{2}R^4\Lambda^4 - \frac{2\sqrt{3}}{9}R^5\Lambda^5 + \mathcal{O}(R^6\Lambda^6) \right] \\ \text{Im}Z_2^{\text{triangle}}(R) &= \frac{32}{\sqrt{3}}\Lambda^2 L_3 \left[R^2\Lambda^2 - \frac{1}{2}R^4\Lambda^4 + \frac{2\sqrt{3}}{9}R^5\Lambda^5 + \mathcal{O}(R^6\Lambda^6) \right].\end{aligned}\quad (5.81)$$

Notice that the leading term represents the density at the origin multiplied by the area of the triangle, and that there is no term of the first or third degree in R . The effective value of Z charge is

$$Z_{\text{eff}}^{\text{triangle}}(R) = \frac{64}{\sqrt{3}}R^2\Lambda^4 L_3 + \mathcal{O}(R^6\Lambda^6). \quad (5.82)$$

We can also choose a circle of radius R as a domain of integration. For small R ($R\Lambda \ll 1$) we obtain

$$\begin{aligned}\text{Re}Z_1^{\text{circle}}(R) &= -\frac{32\pi}{9}\Lambda^2 L_3 \left[R^2\Lambda^2 - \frac{1}{4}R^4\Lambda^4 + \mathcal{O}(R^6\Lambda^6) \right] \\ \text{Im}Z_2^{\text{circle}}(R) &= \frac{32\pi}{9}\Lambda^2 L_3 \left[R^2\Lambda^2 - \frac{1}{4}R^4\Lambda^4 + \mathcal{O}(R^6\Lambda^6) \right].\end{aligned}\quad (5.83)$$

The leading term is again given by the densities at the origin multiplied by the area of the circle. The effective value of the Z charge is

$$Z_{\text{eff}}^{\text{circle}}(R) = \frac{64\pi}{9}\Lambda^2 L_3 \left[R^2\Lambda^2 - \frac{1}{4}R^4\Lambda^4 + \mathcal{O}(R^6\Lambda^6) \right]. \quad (5.84)$$

A numerical evaluation is needed for large R . We compare the effective Z value evaluated for triangle, inscribed circle and circumscribed circle in Fig. 9. As $R \rightarrow \infty$, the asymptotic slope of $Z_{\text{eff}}^{\text{ins.circle}}(R)$ for inscribed circle converges to the same value as that for the triangle. In the case of the circumscribed circle, the Z_{eff} becomes twice as large as those of the other cases for large R , since the total length of the walls is twice as long as those of the other cases.

5.2.3 Energy of the junction

Since our exact solution satisfies the BPS equation corresponding to $H = H_{\text{II}}$, the energy of the junction is obtained by adding Y_3 and Z_{eff} together $H = Z_{\text{eff}} + Y_3 = -\text{Re}Z_1 + \text{Im}Z_2 + Y_3$.

Firstly we choose the triangle region whose inscribed circle has radius R . For large R ($R\Lambda \gg 1$), the energy is

$$H_{\text{triangle}}(R) = 24\Lambda^3 L_3 R - 2\sqrt{3}\Lambda^2 L_3 + \sqrt{3} \left(5\pi - \frac{16}{3} \right) \Lambda^2 L_3 e^{-\sqrt{3}R\Lambda} + \mathcal{O}(e^{-2\sqrt{3}R\Lambda}). \quad (5.85)$$

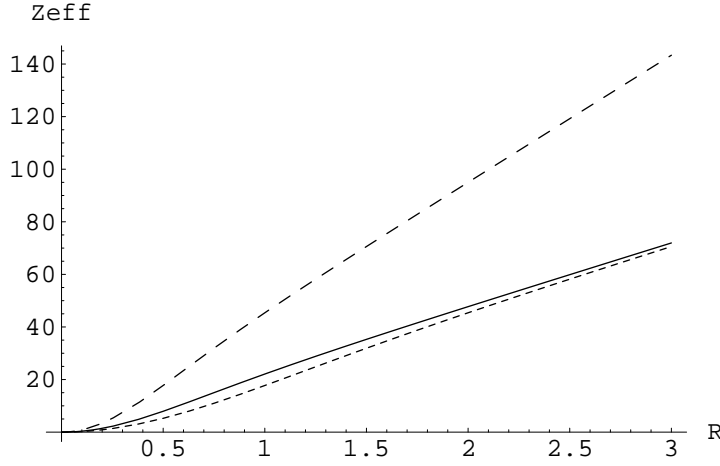


Figure 9: $Z_{\text{eff}}(R)$ evaluated for the triangle (solid line), the inscribed circle of the radius R (short dashed line), and circumscribed circle (long dashed line).

The first linear term can be regarded as the contribution from the walls and the second constant term can be regarded as the contribution from the junction at the center. For small R ($R\Lambda \ll 1$), the energy is

$$H_{\text{triangle}}(R) = \frac{56}{\sqrt{3}}\Lambda^2 L_3 \left[R^2 \Lambda^2 + \frac{1}{7}R^4 \Lambda^4 + \frac{4\sqrt{3}}{315}R^5 \Lambda^5 + \mathcal{O}(R^6 \Lambda^6) \right]. \quad (5.86)$$

In the case of the circle of radius R , the energy is given for small R ($R\Lambda \ll 1$) as

$$H_{\text{circle}}(R) = \frac{56\pi}{9}\Lambda^2 L_3 \left[R^2 \Lambda^2 - \frac{3}{14}R^4 \Lambda^4 + \mathcal{O}(R^6 \Lambda^6) \right]. \quad (5.87)$$

The energy of the triangle region is compared to those of inscribed and circumscribed circles in Fig. 10. For large R ($R\Lambda \gg 1$), the energy H reduces to Z_{eff} .

Finally we plot the θ -dependence of the energy and charges that are obtained by integrating the densities from $r = 0$ to $r = R$ with θ fixed (see Fig. 11). In each figure the energy H (solid line) is the sum of the Z_{eff} (short dashed line) and Y_3 (long dashed line) and Z_3 symmetry is manifest in their θ -dependence. In Fig. 11(a), all the quantities are almost uniform in θ near the junction at the center, reflecting the fact that the junction is a string-like object and symmetric around the x^3 axis. As we move away from the origin, main contribution comes from the direction of the walls (in our case $-\pi/2$, $\pi/6$, and $5\pi/6$) (see Fig. 11(b) and (c)). As R grows, Y_3 disappears and the energy H approaches Z_{eff} (see Fig. 11(d)).

Acknowledgments

One of the authors (H.O.) gratefully acknowledges support from the Iwanami Fujukai Foundation. This work is supported in part by Grant-in-Aid for Scientific Research from the Japan Ministry

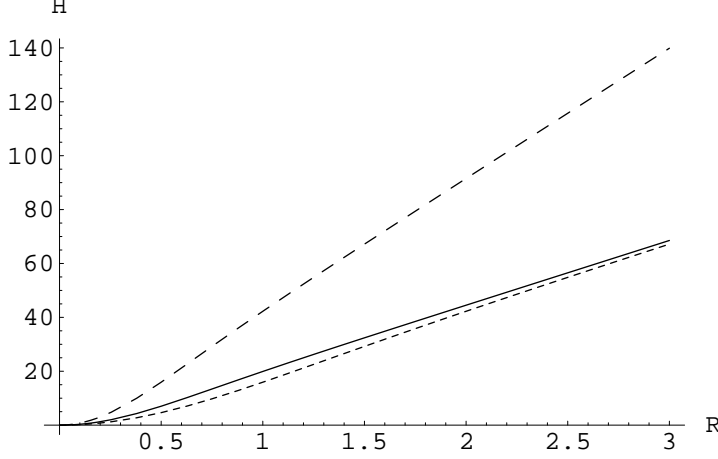


Figure 10: The energy of the junction configuration $H(R)$ evaluated for the triangle (solid), inscribed circle of radius R (short dashed line) and circumscribed circle (long dashed line).

of Education, Science and Culture for the Priority Area 291 and 707.

A Fermionic contributions to central charges

We shall derive the central charges including fermionic contributions in the case of a general Wess-Zumino model with an arbitrary superpotential \mathcal{W} . For simplicity, Kähler metric is assumed to be minimal $K_{ij^*} = \delta_{ij^*}$.

$$\begin{aligned} \mathcal{L} = & -\partial_\mu A^{*j} \partial^\mu A^j + F^{*j} F^j + \frac{i}{2} \partial_\mu \bar{\psi}^j \bar{\sigma}^\mu \psi^j - \frac{i}{2} \bar{\psi}^j \bar{\sigma}^\mu \partial_\mu \psi^j \\ & + F^j \frac{\partial \mathcal{W}}{\partial A^j} - \frac{1}{2} \psi^i \psi^j \frac{\partial \mathcal{W}}{\partial A^i \partial A^j} + F^{*j} \frac{\partial \mathcal{W}^*}{\partial A^{*j}} - \frac{1}{2} \bar{\psi}^i \bar{\psi}^j \frac{\partial \mathcal{W}^*}{\partial A^{*i} \partial A^{*j}}. \end{aligned} \quad (\text{A.1})$$

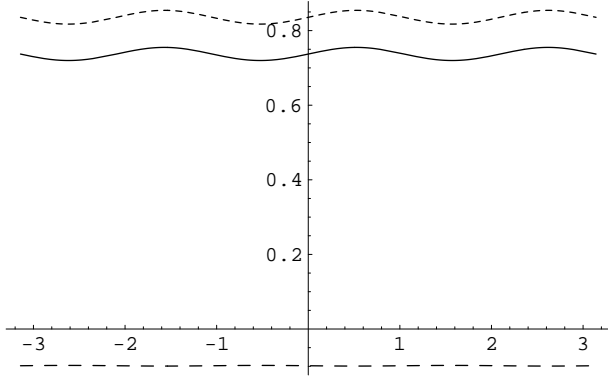
We have added a surface term to Eq.(2.3) to make the variational principle meaningful. This is the starting Lagrangian to derive central charges and we will not neglect any total divergences from now on. The canonical supercurrent is found to be

$$\begin{aligned} J_\alpha^\mu &= \sqrt{2} (\sigma^\nu \bar{\sigma}^\mu \psi^i)_\alpha \partial_\nu A^{i*} + i\sqrt{2} (\sigma^\mu \bar{\psi}^i)_\alpha F^i \\ &= \sqrt{2} (\sigma^\nu \bar{\sigma}^\mu \psi^i)_\alpha \partial_\nu A^{i*} - i\sqrt{2} (\sigma^\mu \bar{\psi}^i)_\alpha \frac{\partial \mathcal{W}^*}{\partial A^{*i}} \end{aligned} \quad (\text{A.2})$$

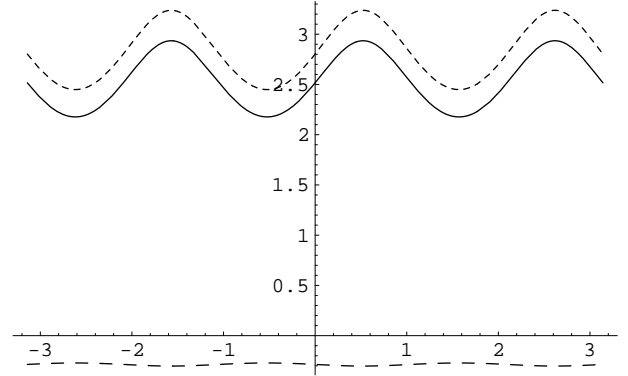
$$\begin{aligned} \bar{J}^{\mu\dot{\alpha}} &= \sqrt{2} (\bar{\sigma}^\nu \sigma^\mu \bar{\psi}^i)^{\dot{\alpha}} \partial_\nu A^i + i\sqrt{2} (\bar{\sigma}^\mu \psi^i)^{\dot{\alpha}} F^{i*} \\ &= \sqrt{2} (\bar{\sigma}^\nu \sigma^\mu \bar{\psi}^i)^{\dot{\alpha}} \partial_\nu A^i - i\sqrt{2} (\bar{\sigma}^\mu \psi^i)^{\dot{\alpha}} \frac{\partial \mathcal{W}}{\partial A^i} \end{aligned} \quad (\text{A.3})$$

The canonical energy momentum tensor is given by

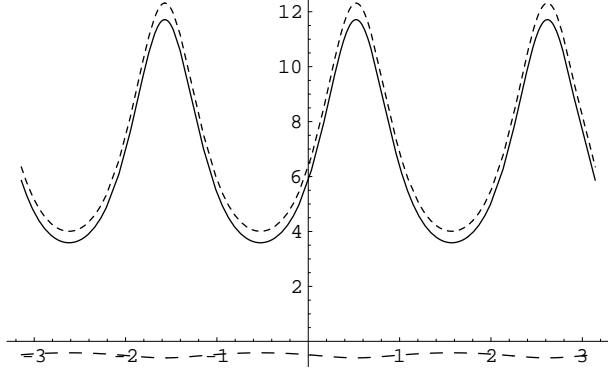
$$T^{\mu\nu} = \partial^\mu A^j \partial^\nu A^{*j} + \partial^\mu A^{*j} \partial^\nu A^j + \frac{i}{2} \bar{\psi}^j \bar{\sigma}^\mu \partial^\nu \psi^j + \frac{i}{2} \psi^j \sigma^\mu \partial^\nu \bar{\psi}^j \quad (\text{A.4})$$



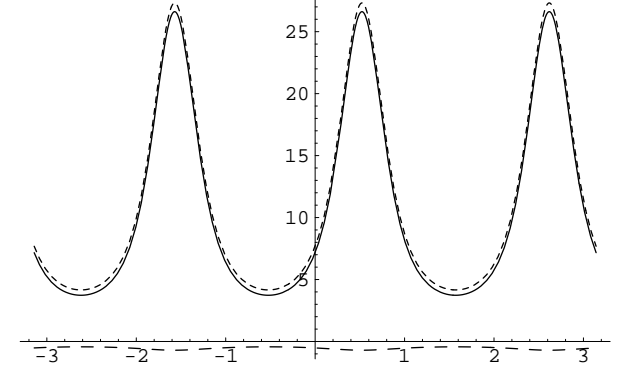
(a) $R\Lambda = 0.5$ case



(b) $R\Lambda = 1$ case



(c) $R\Lambda = 2$ case



(d) $R\Lambda = 3$ case

Figure 11: The θ -dependence of the energy and charges that are obtained by integrating the densities over the radial direction up to R with θ fixed. In each figure horizontal axis denotes θ , and solid, short dashed and long dashed lines correspond to H , Z_{eff} and Y_3 respectively.

$$+g^{\mu\nu} \left[-\partial_\lambda A^{*j} \partial^\lambda A^j - \left| \frac{\partial \mathcal{W}}{\partial A^j} \right|^2 + \frac{i}{2} \partial_\lambda \bar{\psi}^j \bar{\sigma}^\lambda \psi^j - \frac{i}{2} \bar{\psi}^j \bar{\sigma}^\lambda \partial_\lambda \psi^j - \frac{1}{2} \psi^i \psi^j \frac{\partial \mathcal{W}}{\partial A^i \partial A^j} - \frac{1}{2} \bar{\psi}^i \bar{\psi}^j \frac{\partial \mathcal{W}^*}{\partial A^{*i} \partial A^{*j}} \right].$$

Canonical quantization gives (anti-) commutation relations

$$[A^i(x), \partial_0 A^{*j}(y)]_{x^0=y^0} = i\delta^3(x-y)\delta^{ij}, \quad \left\{ \psi_\alpha^i(x), \bar{\psi}_\beta^j(y) \right\}_{x^0=y^0} = -\delta^3(x-y)\delta^{ij}\sigma_{\alpha\dot{\beta}}^0. \quad (\text{A.5})$$

The anticommutator between supercharges of the same chirality gives the supersymmetry algebra (2.1) with the central charge Z_k in Eq.(2.4)

$$Z_k = 2 \int d^3x \partial_k \mathcal{W}^*(A^*) \quad (\text{A.6})$$

which turns out to have only bosonic contributions. The anticommutator between supercharges of the opposite chirality gives the supersymmetry algebra (2.2) with the central charge Y_k

$$Y_k = i\epsilon^{knm} \int d^3x \partial_n \left(A^{*j} \partial_m A^j - \frac{1}{2} \bar{\psi}^j \bar{\sigma}_m \psi^j \right), \quad \epsilon^{123} = 1, \quad (\text{A.7})$$

which has both bosonic and fermionic contributions.

B Gamma matrices and fermion mode equations

In order to separate variables (x^1, x^2) and (x^0, x^3) for spinors, it is most convenient to use a gamma matrix representation where the direct product structure of 2×2 matrices in (x^1, x^2) and (x^0, x^3) becomes manifest. One such representation is

$$\gamma^0 = \rho^1, \quad \gamma^3 = i\rho^2, \quad \gamma^1 = i\sigma^1\rho^3, \quad \gamma^2 = i\sigma^2\rho^3, \quad (\text{B.1})$$

where σ^a are Pauli matrices acting on 2×2 matrices and ρ^a acting on indices of blocks of these 2×2 matrices. The four component spinor can be decomposed into a pair of two component spinors ξ and χ in $0+1$ dimensions

$$\psi = \begin{bmatrix} \xi \\ i\chi \end{bmatrix}, \quad (\text{B.2})$$

The B matrix for $1+3$ dimensions can be defined as a product of B matrices $B^{(1)}$ for $1+1$ dimensions and $B^{(2)}$ for $0+2$ dimensions

$$B = B^{(1)} B^{(2)}, \quad B^{(1)} = \rho^3, \quad B^{(2)} = -i\sigma^1. \quad (\text{B.3})$$

The Majorana condition for the $1+3$ dimensional spinor and the pseudo-Majorana condition for the $0+2$ dimensional spinor are given by

$$\psi = B\psi^*, \quad \xi = B^{(2)}\xi^*, \quad \chi = B^{(2)}\chi^*, \quad (\text{B.4})$$

which implies $\xi_1 = -i\xi_2^*$ for components of the two component spinor $\xi = (\xi_1, \xi_2)^T$, and similarly for χ .

The Dirac equation for four component fermions in the general Wess-Zumino model reads

$$-i\gamma^\mu \partial_\mu \psi^i - \left(\frac{\partial^2 \mathcal{W}}{\partial A^i \partial A^j} \frac{1 + i\gamma^5}{2} + \frac{\partial^2 \mathcal{W}^*}{\partial A^{*i} \partial A^{*j}} \frac{1 - i\gamma^5}{2} \right) \psi^j = 0. \quad (\text{B.5})$$

The mode equation in x^1, x^2 space is defined in terms of two component spinors ξ_n^j and χ_n^j

$$\begin{aligned} \left[\delta^{ij} (\sigma^1 \partial_1 + \sigma^2 \partial_2) - \frac{\partial^2 \mathcal{W}}{\partial A^i \partial A^j} \frac{1 - \sigma^3}{2} - \frac{\partial^2 \mathcal{W}^*}{\partial A^{*i} \partial A^{*j}} \frac{1 + \sigma^3}{2} \right] \xi_n^j &= -m_n^{(1)} \chi_n^i, \\ \left[-\delta^{ij} (\sigma^1 \partial_1 + \sigma^2 \partial_2) - \frac{\partial^2 \mathcal{W}}{\partial A^i \partial A^j} \frac{1 + \sigma^3}{2} - \frac{\partial^2 \mathcal{W}^*}{\partial A^{*i} \partial A^{*j}} \frac{1 - \sigma^3}{2} \right] \chi_n^j &= -m_n^{(2)} \xi_n^i. \end{aligned} \quad (\text{B.6})$$

The two component spinors ξ_n^i, χ_n^i satisfy the pseudo-Majorana condition (B.4). Then we find that mass eigenvalues are real

$$m_n^{(1)} = (m_n^{(1)})^*, \quad m_n^{(2)} = (m_n^{(2)})^*. \quad (\text{B.7})$$

We can make a separation of variables for the Dirac equation (B.5) by means of real fermionic fields c_n and b_n

$$\psi^i = \sum_n \begin{bmatrix} c_n(x^0, x^3) \xi_n(x^1, x^2) \\ i b_n(x^0, x^3) \chi_n(x^1, x^2) \end{bmatrix}. \quad (\text{B.8})$$

Using these mode functions we find that the fermion fields $(c_n, i b_n)^T$ satisfy the Dirac equation in $1 + 1$ dimensions in Eq.(3.46).

This representation can be related to the usual Weyl representation in ref. [20] by the following unitary matrix U

$$U = \frac{1 - \sigma^3}{2} \rho^3 + \frac{1 + \sigma^3}{2} \rho^2, \quad \gamma_{\text{Weyl}}^\mu = U^\dagger \gamma^\mu U, \quad B_{\text{Weyl}} = U^\dagger B U^* = \sigma^2 \rho^2. \quad (\text{B.9})$$

The two component spinor in the Weyl representation is related to the components of the four component spinor (B.2) in the representation (B.1) in this appendix as

$$\begin{bmatrix} \psi_\alpha \\ \bar{\psi}^{\dot{\alpha}} \end{bmatrix}_{\text{Weyl}} = \begin{bmatrix} \chi_1 \\ \xi_2 \\ i\xi_1 \\ -i\chi_2 \end{bmatrix}. \quad (\text{B.10})$$

Thus we obtain the mode equation (3.41)– (3.44) in the Weyl representation.

References

- [1] N. Arkani-Hamed, S Dimopoulos, and G. Dvali, *Phys. Lett.* **B429** (1998) 263, hep-ph/9803315; I. Antoniadis, N. Arkani-Hamed, S Dimopoulos, and G. Dvali, *Phys. Lett.* **B436** (1998) 257, hep-ph/9804398.

- [2] L. Randall and R. Sundrum, *Phys. Rev. Lett.* **83** (1999) 3370, hep-ph/9905221; *Phys. Rev. Lett.* **83** (1999) 4690, hep-th/9906064.
- [3] N. Arkani-Hamed, S. Dimopoulos, G. Dvali, and N. Kaloper, *Phys. Rev. Lett.* **84** (2000) 586, hep-th/9907209; C. Csaki and Y. Shirman, *Phys. Rev.* **D61** (2000) 024008, hep-th/9908186; A. E. Nelson, “A new angle on intersecting branes in infinite extra dimensions”, hep-th/9909001.
- [4] K. Behrndt and M. Cvetič, “Supersymmetric domain wall world from $D = 5$ simple gauged supergravity”, hep-th/9909058; K. Skenderis and P. Townsend, *Phys. Lett.* **B468** (1999) 46, hep-th/9909070; A. Chamblin and G. W. Gibbons, ”Supergravity on the Brane”, hep-th/9909130; O. DeWolfe, D. Z. Freedman, S. S. Gubser, and A. Karch, “Modeling the fifth dimension with scalars and gravity”, hep-th/9909134.
- [5] E. Bogomol’nyi, *Sov. J. Nucl. Phys.* **24** (1976) 449; M. K. Prasad and C. H. Sommerfield, *Phys. Rev. Lett.* **35** (1975) 760.
- [6] E. Witten and D. Olive, *Phys. Lett.* **B78** (1978) 97.
- [7] E. R. C. Abraham and P. K. Townsend, *Nucl. Phys.* **B351** (1991) 313.
- [8] G. Dvali and M. Shifman, *Phys. Lett.* **B396** (1997) 64, hep-th/9612128; *Nucl. Phys.* **B504** (1997) 127, hep-th/9611213.
- [9] A. Kovner, M. Shifman, and A. Smilga, *Phys. Rev.* **D56** (1997) 7978, hep-th/9706089; A. Smilga and A. Veselov, *Phys. Rev. Lett.* **79** (1997) 4529, hep-th/9706217; B. de Carlos and J. M. Moreno, *Phys. Rev. Lett.* **83** (1999) 2120, hep-th/9905165; G. Dvali, G. Gabadadze, and Z. Kakushadze, *Nucl. Phys.* **B562** (1999) 158, hep-th/9901032.
- [10] V. Kaplunovsky, J. Sonnenschein, and S. Yankielowicz, *Nucl. Phys.* **B552** (1999) 209, hep-th/9811195.
- [11] V.A. Rubakov and M.E. Shaposhnikov, *Phys. Lett.* **B125** (1983) 136.
- [12] B. Chibisov and M. Shifman, *Phys. Rev.* **D56** (1997) 7990, hep-th/9706141.
- [13] G. Gibbons and P. K. Townsend, *Phys. Rev. Lett.* **83** (1999) 1727, hep-th/9905196.
- [14] S. M. Carroll, S. Hellerman and M. Trodden, *Phys. Rev.* **D61** (2000) 065001, hep-th/9905217.
- [15] A. Gorsky and M. Shifman, *Phys. Rev.* **D61** (2000) 085001, hep-th/9909015.
- [16] P. M. Saffin, *Phys. Rev. Lett.* **83** (1999) 4249, hep-th/9907066; D. Bazeia and F. A. Brito, *Phys. Rev. Lett.* **84** (2000) 1094, hep-th/9908090.
- [17] H. Oda, K. Ito, M. Naganuma and N. Sakai, *Phys. Lett.* **B471** (1999) 148, hep-th/9910095.
- [18] P. Townsend, *PASCOS/Hopkins* (1995) 0271, hep-th/9507048.

- [19] P. Townsend, *Class. Quant. Grav.* **17** (2000) 1267, hep-th/9911154.
- [20] J. Wess and J. Bagger, “Supersymmetry and Supergravity”, 1991, Princeton University Press.
- [21] D. Binosi and T. tel Veldhuis, *Phys. Lett.* **B476** (2000) 124, hep-th/9912081; D. Bazeia and F.A. Brito, “Bags, junctions, and networks of BPS and non-BPS defects”, hep-th/9912015.
- [22] M. Shifman and T. tel Veldhuis, “Calculating the tension of domain wall junctions and vortices in generalized Wess-Zumino models”, hep-th/9912162.
- [23] S. M. Carroll, S. Hellerman, and M. Trodden, “BPS domain wall junctions in large extra dimensions”, hep-th/9911083; N. Arkani-Hamed, S Dimopoulos, G. Dvali, and N. Kaloper, “Manyfold universe”, hep-ph/9911386; S. Nam, *JHEP.* **0003** (2000) 005, hep-th/9911104; I. Bakas, A. Brandhuber, and K. Sfetsos, “Domain walls of gauged supergravity, M-branes and algebraic curves”, hep-th/9912132; M. Cvetič, H. Lü, and C. N. Pope, “Domain walls and massive gauged supergravity potentials”, hep-th/0001002; C. Csaki, J. Erlich, T. J. Hollowood, and Y. Shirman, “Universal aspects of gravity localized on thick branes”, hep-th/0001033; R. Kallosh and A. Linde, *JHEP.* **0002** (2000) 005, hep-th/0001071; S. Nam and K. Olsen, “Domain wall junctions in supersymmetric field theories in $D = 4$ ”, hep-th/0002176; R. Altendorfer, J. Bagger, and D. Nemeschansky, “Supersymmetric Randall-Sundrum scenario”, hep-th/0003117; N. Alonso-Alberca, P. Meessen, and T. Ortin, “Supersymmetric brane-worlds”, hep-th/0003248; J. P. Gauntlett, G. W. Gibbons and P. K. Townsend, “Intersecting domain walls in MQCD”, hep-th/0004136.